Discover Food

Discover

Review

Factors influencing droplet size in pneumatic and ultrasonic atomization and its application in food processing

Mariola Camacho-Lie[1] · Oscar Antonio-Gutiérrez[2] · Andrea Selene López-Díaz[2] · Aurelio López-Malo[1] · Nelly Ramírez-Corona[1]

Received: 1 August 2023 / Accepted: 29 November 2023
Published online: 07 December 2023

Abstract
Droplet size has significant scientific and industrial relevance in the effectiveness of atomization for several applications in the chemical, pharmaceutical, and food industries. This technology is widely employed in the food industry for processes such as spray drying, microencapsulation, edible coatings, and food disinfection, among others. This work comprehensively reviews the effect of liquid properties and equipment operating factors influencing droplet size in pneumatic and ultrasonic atomization. The discussion on the atomization theories includes the different models for estimating droplet size as a function of selected variables for both processes. The different model approaches are reviewed, focusing on their advantages, disadvantages, applications, and limitations. Furthermore, selected models were employed to carry out different sensitivity analyses showing the effect of variables related to the liquid properties, the type and characteristics of the atomizers, and the operating conditions, allowing the reader to appreciate the most critical factors in both atomization systems.

Keywords Droplet size · Atomization · Pneumatic · Ultrasound · Food processing

1 Introduction

Liquid atomization (Fig. 1) is the disintegration of a liquid film that comes out on a solid surface subjected to a sufficient surface disturbance in the normal direction. The competition between disruptive (like kinetic energy, friction, gravity, interface shearing, and pressure fluctuation) and cohesive (like shear resistance, the surface tension of liquids, and extensional resistance) forces on the liquid surface induce fluctuations and disturbances in the liquid, separating it from the surface and splits into small droplets like a mist in the gas phase [1–3]. The initial process of disintegration or break-up is defined as primary atomization, while the second atomization occurs when numerous larger droplets produced in the primary atomization can be unstable, thus reducing to smaller sizes [2, 4].

Atomization quality can be described in terms of mean drop size and distribution, and it depends on the flow conditions, liquid properties, gas properties, atomizer dimensions (nozzle or injector), and environmental conditions [4]. Heat and mass transfer efficiency improve by decreasing the droplet's size due to increased surface area [6]. Atomization applications in the food industry are vast. Some examples of the use of this technology are spray drying and microencapsulation. Spray drying is commonly used to preserve foods and bioactive compounds. In addition,

✉ Nelly Ramírez-Corona, nelly.ramirez@udlap.mx | [1]Departamento de Ingeniería Química, Alimentos y Ambiental, Universidad de las Américas Puebla, San Andrés Cholula, 72810 Puebla, México. [2]Instituto Politécnico Nacional, Centro Interdisciplinario de Investigación para el Desarrollo Integral Regional Unidad Oaxaca, Hornos 1003, Santa Cruz Xoxocotlán, 71230 Oaxaca, México.

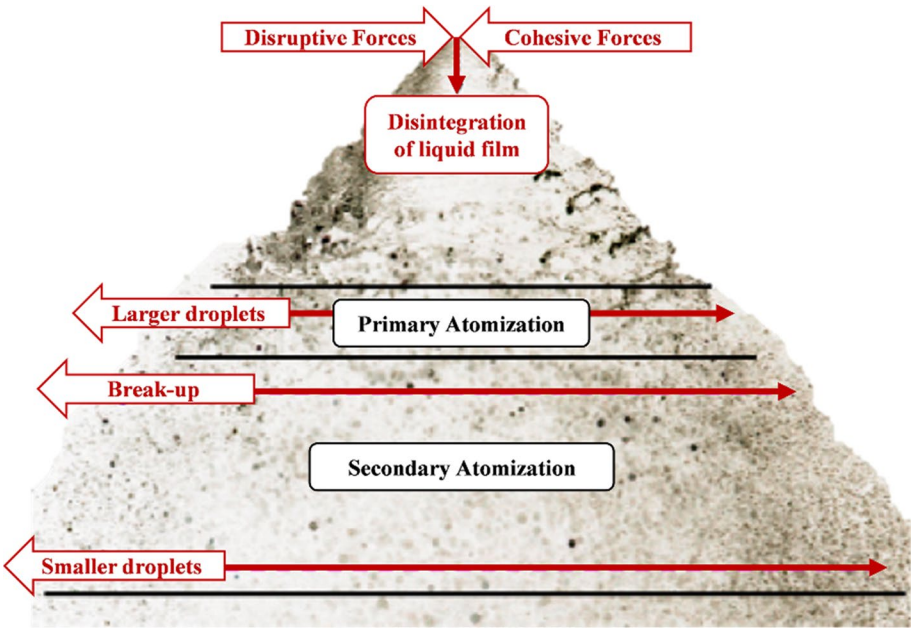

Fig. 1 Schematic of liquid atomization. Adapted from Movahednejad et al. [5]

atomization has been combined with conventional preservation methods, antimicrobial agents, or other non-thermal treatments to improve the antimicrobial effect. In the second example, microencapsulation has several advantages with its application to food ingredients, including reduced oxidation, improved stability, and improved sensory attributes. Besides, probiotics are spray-dried for long-term storage conditions for food applications [7–9]. In the following section, such applications are described.

2 Applications of atomization in food processing technologies

In the food industry, spray technology is used in many stages during food processing, depending on the product type. Some of its applications include coatings, flavorings, antimicrobial agents and mold inhibitors, cleaning tanks, equipment and floors, spray drying, and air blowing, among others. Depending on the characteristics of the food matrix to be processed and the desired product, each type of atomization has its advantages; for instance, ultrasonic atomization is very suitable for the drying of viscous, thick and/or abrasive liquid feed products, while pneumatic atomization has low costs and low energy consumption [10]. Table 1 summarizes selected pneumatic and ultrasonic atomization applications in food processing [11–19].

The main applications of atomization are spray drying, edible coatings, encapsulation, and disinfection. Droplet size's influence on these applications is discussed in depth in the following sections.

2.1 Spray drying

Spray drying is a process of water evaporation, using hot air to stabilize liquid solutions and suspensions to produce powders [20, 21]. This processing technique offers the advantages of relatively low temperatures and short particle residence times (5–100 s). For this reason, some properties of food, such as flavor, color, and nutrients, can be retained [21, 22].

Atomization is a key element of the spray-drying process, and it is defined as the disintegration of a liquid into droplets in a surrounding gas by an atomizer. These droplets, through evaporation of water in the main dryer chamber, become individual powder particles during the spray-drying process [10, 23].

The effect of atomization in spray drying has been widely studied. The influence of spray drying conditions on the processing performance and physicochemical properties of sugarcane juice (JCP) and whey protein concentrate (WPC) combined system were evaluated by Uscategui et al. [24]. According to their results, larger particles are formed as the atomization rate decreases (with low WPC contribution). This fact is probably because low velocities produce larger droplets that directly influence the particle size of the powder, which is especially evident in solutions with higher solid

Table 1 Some applications of pneumatic and ultrasonic atomization in food processing

Technology	Application	Material	Purpose	Product
Ultrasonic atomization	Spray drying	Liquid foods	Dry powder	Blueberries [11] Green banana starch [12]
Ultrasonic atomization and UV treatment	Disinfection	Liquid foods	Microbial inactivation	Tangerine and grapefruit juices [13]
Ultrasonic vacuum atomization	Spray drying Micro-encapsulation	Liquid foods Probiotics	Dry powder	*Lactobacillus casei subsp. paracasei* LMG P-21380 [14] Honey [15]
Ultrasonic spray-freeze drying	Micro-encapsulation	Liquid foods Probiotics	Dry powder	Microbial transglutaminase [16]
Pneumatic atomization	Edible Coatings	Fresh and processed food products	Spray coating	Bakery products [17]
Pneumatic atomization	Encapsulation Spray drying	Emulsions Liquid foods	Active ingredients, aroma, and coloring compounds. Dry powder	Bioactive ingredients [18] Skim milk powder [19]

contents. The contrary effect was observed by Finney et al. [25], with increasing the spray-drying atomization airflow rate, the resulting droplets decreased, producing powder particles with smaller sizes.

On the other hand, it was demonstrated that the viscosity of the feed solution is an important parameter to consider in the spray drying process, since the mean size of the atomized droplets varies directly to the viscosity of the liquid [26]. Also, the droplet size produced during atomization affects the resulting powder. Too large drops may lead to incomplete drying, resulting in stickiness and reduced storage stability, while too small drops can lead to thermal degradation reactions within the fine fraction or to the formation of undesired fine particles [27–29].

Mensink et al. [30] observed that the obtention of particles with the largest average size in a higher concentration of inulin might be related to this carbohydrate's capability to form solutions with high viscosity. Then, as the viscosity of the feed solution increased, the droplets formed during the atomization process also increased, and larger powder particles were obtained. Higher feed viscosity by increasing the droplet size produced during atomization caused lower bulk and tapped density of powders [31]. Also, viscosity affects other properties, including flowability, rehydration, and solubility [32].

Viscosity has been widely studied to improve milk drying. Different properties and variables, such as total solids or temperature, significantly impact milk viscosity [33]. The droplet size produced during milk atomization influences the final characteristics of the powder. Outsized droplets can cause incomplete drying, resulting in stickiness and decreased stability during storage. [27], whereas tiny droplets can cause thermal degradation reactions [28], unwanted fine particles may form [29]. In the food industry, maximum yield can be obtained by concentrating the milk until high total solid concentrations are achieved, which also helps save energy [34].

In the case of milk, the drop and size distribution are determined by the nozzle type and its process parameters [35]. Pressure-swirl nozzles have been used in the milk industry because of their economic benefit and feasibility [36]. Pressure-swirl atomizers operate by applying pressure, which generates swirl flow that converts the liquid's potential energy into kinetic energy, resulting in relative velocity differences between the spray stream and the air outside [33]. Viscosity, density, surface tension, the type of atomizer, and its operating conditions are the most critical variables controlling the droplet size [37]. Then, controlling the formation of desirable droplets is fundamental for the spray drying process optimization.

Habtegebriel et al. [38] reported the influence of the viscosity of camel milk during its atomization. Camel milk presented lower viscosity than cow milk; therefore, atomization at higher total solids would be more appropriate, resulting in less water evaporation and improving the drying process. Also, when using a pressure-swirl nozzle, bigger droplets with narrower spans are gotten at 100 bar and 20 °C. Saha et al. [39] evaluated the characteristics of the groundnut milk powder obtained by optimizing inlet air temperature, pressure, and feed pump velocity during spray drying. Their study indicates that powders with low moisture content can be obtained at higher inlet temperature and pressure. The bulk density and dispersibility of the powders increase when atomization pressure increases. The evaluation of these properties becomes crucial depending on the packaging material specifications and the product's desired characteristics, including reconstitution properties.

Moreover, spray drying of emulsions is a typical process used in the food industry. This process is implemented to produce dairy powders, encapsulated aroma, and coloring compounds, among other products [40]. The droplet size of the resulting powder determines the final product's characteristics and stability. The first step of spray drying an emulsion is atomization. Primary atomization is the initial process of liquid disintegration [23]. Nevertheless, some bigger droplets obtained during the primary atomization, occurring at the nozzle exit, might be unstable [2]; a secondary process called "secondary atomization" is needed to reduce the droplet size [41].

Previous studies have demonstrated that droplet distribution changes can occur during spray drying [42, 43]. Taboada et al. [40] investigated the influence of the emulsifier systems as whey protein isolate (WPI) with lecithin, mono-and diglycerides (MoDi), and citrem. According to their results, oil droplet coalescence is detected for WPI/Citrem and WPI/MoDi systems. Similar results were reported by adding monoglycerides and fatty acid esters to protein-stabilized emulsions [44, 45]. However, other studies propose that coalescence can be avoided by adding WPI/Lecithin during the drying step. Also, chickpea protein (CP) exhibits good functional properties, including high emulsifying potential and encapsulating ability, since this protein allows the development of thick viscoelastic films around oil droplets, which improves their stability [23].

Ultrasonic nozzle technology has been implemented for spray-drying processes since it helps atomize uniform droplets, protecting the bioactive compounds [46]. In this process, a thin liquid film is formed on the resonant surface by introducing the liquid into the feed capillary at the nozzle's tip [9]. Then, ultrasonic vibrations are induced through the liquid medium when the liquid is in contact with the piezoelectric disk surface; atomization occurs when vibrations are

sufficiently higher, beyond the liquid surface tension. The size of the formed droplets is linked with the liquid viscosity, surface tension, density, and concentration [47]. Tatar Turan et al. [46] studied the performance of an ultrasonic spray nozzle on coating materials (made from carbohydrates and proteins) for microencapsulation of blueberry extract. Results showed that the ultrasonic atomizer frequency is the key factor affecting the droplet size, which decreases by increasing the frequency.

Ultrasonic spray drying can be applied in food manufacturing to attain a uniform distribution of dried particles with specific characteristics. Although this technique has several advantages, it has been applied only for a few applications, such as microencapsulation. Although spray drying is a standard process in the dairy industry, the industrial implementation of ultrasound for spray drying is limited because the current large-scale reactors are not economically suitable [9].

2.2 Edible coatings

The edible coating is a thin film of edible material covering the food surface as protective coating, which can be consumed with the food product. The coating's effectiveness strongly depends on the application method. Those films can be applied in liquid form by immersing the food product in a film-forming solution or spraying the solution on the food surface [48]. The deposition methods of coatings depend on the type of food to be coated, the surface characteristics, and the aim of the coating [49]. The spraying method has been applied to many food products, including bell pepper [50], oranges [51], okra [52], cassava [53], fruit-based salads [54], and different types of meat [55].

One method to spray solutions is the electro-spray system, which has several advantages over mechanical spray atomizers. Lefebvre and McDonell [36] demonstrated that electrostatic spraying increases the application efficiency up to 80%, reducing the spray dosage to 50%. Also, this type of coating reduces the processing time required for coating fruits [56]. When electrostatic sprayers are used, atomized liquid particles receive the charge at the nozzle end, following the trajectory in the direction of the adjacent grounded object, thus forming a uniform coating due to the effect of charged particles [36]. In this technique, the liquid flowrate and the capillary nozzle voltage can affect droplet generation and size [56].

Khan et al. [57] studied the atomization behavior of sunflower oil, evaluating the effect of liquid's properties and flowrate of electrostatic spraying. Results showed that sunflower oil's flow rate and conductivity influence droplet size. Also, they observed that charged droplets were randomly placed on both types of surfaces, conductive and non-conductive. Then, the droplets charge significantly affects uniform film formation on target surfaces. Recently, Hanumantharaju et al. [56] developed an electrostatic spray coating device to coat fruits. They observed that the droplet size obtained by the electrostatic spray was reduced, and improved uniformity was attained compared to the standard method. Also, the coating solution requirements were reduced during electrostatic spray coating.

The effectiveness of coatings for food protection depends on the film thickness that can be controlled by adjusting the coating solution's spreading [58]. To control the final droplet size, it is essential to consider many factors, such as liquid properties, spray-nozzle design, and air velocity. Typically, the largest droplet size results from using full-cone nozzles, followed by flat-spray and hollow-cone nozzles. The droplet size is directly influenced by liquid flow rate and spray angle; increasing liquid viscosity decreases the flow rate; consequently, the lowest pressure should be increased to keep an acceptable spraying angle. Conversely, when surface tension increases, the operating pressure minimizes, and the spray angle decreases [59, 60].

2.3 Encapsulation

Intending to protect bioactive substances from the environment and increase their stability until their deferred, directed, or controlled release, encapsulation is the ideal process to protect delicate components by entrapmenting the bioactive core with wall materials [61]. Spray drying is one technique that has achieved high encapsulation efficiency; however, droplet drying is complicated due to broad drop-size distributions and complex airspray mixing patterns [62]. Food powder products with encapsulated oily components produced by spray drying of oil-in-water emulsions can be illustrated by infant formula, instant dairy powder, and products with encapsulated flavors [40]. One of the parameters to consider that determine the efficiency of encapsulation and, consequently, the extent of non-encapsulated material, is the size and stability of the oil droplets [63]. When using high-pressure nozzles, large oil droplets will lead to a decreased encapsulation efficiency; the characteristics of the emulsion and the spray drying conditions are also fundamental [64]. For instance, Taboada, Schäfer, Karbstein, & Gaukel [65] found that the oil droplet break-up is highly dependent on the atomization pressure, as the stresses in the liquid film of the atomizer orifice correlate with the atomization pressure,

concluding that as the oil droplet size in the final product can be responsible for several properties. Zhang et al. [66] evaluate the droplet size distribution during ultrasonic atomization by laser diffraction. Their results indicated that the droplet size distribution varied from a narrow to a wide range with the increasing liquid flow rate. Furthermore, the droplet size did not increase monotonously when the input power and liquid viscosity increased, and it was observed that it gradually increased as the droplets fell due to their aggregation behavior, which led them to conclude that the mean droplet size and size distribution are highly dependent on operating parameters of equipment and liquid physicochemical properties.

2.4 Disinfection and other applications

Pneumatic and ultrasonic atomization have been evaluated to pasteurize some fruit juices in combination with other technologies. Orange, grapefruit, cranberry, and pomegranate juices were processed in a combined ultrasonic and pneumatic atomization system with UVC light. The authors found that the UVC + pneumatic atomization arrangement achieved five decimal reduction cycles. For orange and grapefruit juices, losses of 11% and 14% of ascorbic acid were observed, respectively, while for pomegranate and blueberry juices, the anthocyanin content was reduced by 50% and 40% [67].

Other atomization applications in food processing are used indirectly; for instance, Mohammed et al. [68] evaluated the implementation of an ultrasonic humidifier during cold storage of vegetables and fruits, wherein this equipment helps regulate the relative humidity and preserve their quality. For this type of application, the frequency of the ultrasonic transducer determines the droplet size. The authors concluded that such droplet size improves the humidifier's performance in preserving the fruit quality and reducing the product water loss [68].

In the case of emulsions, electrostatic atomization is a method that functions to encapsulate oil by powder using an electric field, together with an aqueous solution that contains the wall material within the oil phase, wherein increasing the aqueous solution conductivity reduces the droplet size [69–71]. Mori et al. [72] encapsulate soybean oil by this electrostatic atomization technique. The droplet size of the aqueous glycine solution was smaller than that of the taurine aqueous solution. Similarly to the spray drying process, the particle size depends on the droplet size, which decreases with decreasing droplet size.

Electrostatic atomization has also been used to sanitize food products. Mohammadi-Aragh et al. [73] analyzed the effects of various disinfectants on broiler-hatching eggs' bacterial load and microbiome using electrostatic spray. Electrostatic sprayers increase chemical application efficiency by reducing the amount of chemicals and water used, while increasing spray deposition and retention of antimicrobial droplets on the surface of a material [74, 75]. Also, Lee et al. [76] evaluated the application of passion fruit peel extract (PPE) using an electrostatic spraying system to disinfect fresh-cut Lollo Rossa and beetroot. Results indicated that electrostatic spraying of PPE was more effective than washing with PPE. They concluded that electrostatic spraying of PPE can be used as a novel disinfection method since the color and texture of fresh-cut Lollo Rossa leaves during storage were not affected.

3 Type of atomizers

Depending on the liquid feed's properties and product requirements, the basic types of atomizers utilized are rotary, pressure, and pneumatic nozzles. The two most common atomizing devices used in the food industry are centrifugal (rotary) and pressure (nozzle) atomizers, although ultrasonic atomizers offer a viable alternative due to better control of droplet size distribution and a smaller average size [6, 7].

Pneumatic nozzles, also known as twin-fluid or two-substance nozzles, consist of a tube with double-entry flows of air, vapor, and/or liquid, where the feed is atomized by high-velocity air, gas, or steam. The liquid feed can be mixed with the air inside or outside the body of the nozzle (Fig. 2). They are suitable for viscous, thick, and/or abrasive liquid feed products, and create fine particles; but have the highest energy consumption due to the cost of compressed air [10, 36, 77]. The variation of the liquid feed properties modifies the particle size and morphology: a low-viscosity feed will result in small mean droplet size and a high homogeneity, whereas a high-viscosity feed will give rise to a larger mean droplet size and lower homogeneity. The increment of the viscosity and/or surface tension increases the energy required to atomize the spray and the drop size [10, 78, 79].

Otherwise, the ultrasonic atomizer is an electromechanical device consisting of two piezoelectric disks pressed with a support element, where the liquid in a thin layer is spread over the atomization surface and is introduced into capillary

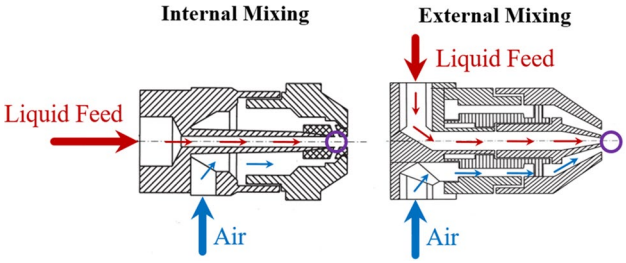

Fig. 2 Pneumatic nozzles with internal and external mixing. Adapted from Písecký [77]

waves of higher frequency than the threshold of human auditory detection (≥ 16 kHz), through vibrating ultrasound (Fig. 3) [6, 10].

Atomization takes place when produced vibrations are higher than the liquid's surface tension. The ultrasound parameters, like power and frequency, and the properties of the liquid (density, viscosity, surface tension, and concentration) define the intensity of the capillary waves. Overall, the ultrasonic nozzle better regulates the processing flow rates and the particle size distribution compared to conventional nozzles [6, 9].

4 Theory of pneumatic atomization. Models for estimation of droplet size

In pneumatic atomization, the resulting forces affecting the atomized liquid are described by the following dimensionless numbers: Reynolds (Re), Eq. (1), Weber (We), Eq. (2), and Ohnesorge (Oh), Eq. (3). All these dimensionless numbers can be computed by using the liquid properties as its density (ρ), velocity (u), dynamic viscosity (μ), and surface tension (σ), as well as the jet diameter during primary atomization or drop diameter during secondary atomization (d_p). Therefore, the droplet diameter can be estimated as a function of the liquid properties, the atomizer geometry, and parameters like the liquid/air flow rate. It is important to notice that most correlations reported in the literature are empirical [2, 47, 79].

$$\mathrm{Re} = \frac{\rho u d_p}{\mu} = \frac{\text{Inertia Forces}}{\text{Viscous Forces}} \tag{1}$$

$$\mathrm{We} = \frac{\rho u^2 d_p}{\sigma} = \frac{\text{Inertia Forces}}{\text{Surface Tension}} \tag{2}$$

$$\mathrm{Oh} = \frac{\sqrt{\mathrm{We}}}{\mathrm{Re}} = \frac{\mu}{\sqrt{\rho \sigma d_p}} = \frac{\text{Viscous Forces}}{\sqrt{(\text{Inertia Forces})(\text{Surface Tension})}} \tag{3}$$

The type of atomizer determines the energy required to form the spray, the size and distribution of the drops, and their trajectory and speed. The mean droplet size and size distribution define the spray characteristics [79]. However, working only with mean or average diameters is more convenient than the complete drop size distribution in mass

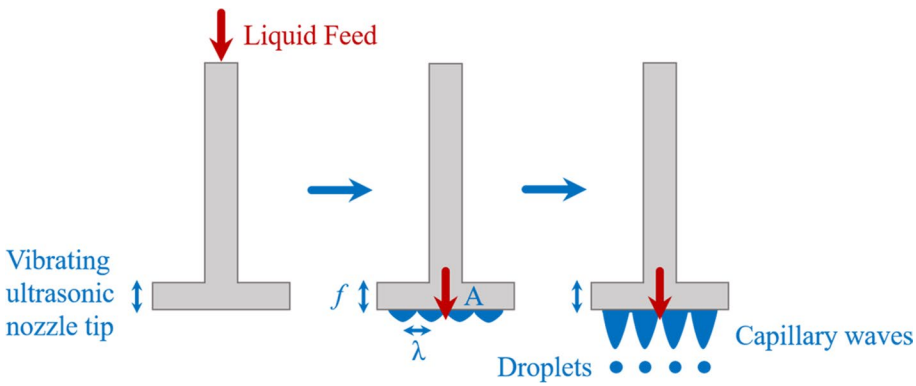

Fig. 3 Formation of droplets by ultrasound atomizer. Adapted from Samborska et al. [6]

Table 2 Mean diameters and their applications [36]

a	b	Order a + b	Symbol	Name of Mean Diameter	Expression	Application
1	0	1	D_{10}	Length	$\frac{\sum N_i D_i}{\sum N_i}$	Comparisons
2	0	2	D_{20}	Surface area	$\left[\frac{\sum N_i D_i^2}{\sum N_i}\right]^{\frac{1}{2}}$	Surface area controlling
3	0	3	D_{30}	Volume	$\left[\frac{\sum N_i D_i^3}{\sum N_i}\right]^{\frac{1}{3}}$	Volume controlling, e.g., hydrology
2	1	3	D_{21}	Surface area-length	$\frac{\sum N_i D_i^2}{\sum N_i D_i}$	Absorption
3	1	4	D_{31}	Volume-length	$\left[\frac{\sum N_i D_i^3}{\sum N_i D_i}\right]^{\frac{1}{2}}$	Evaporation, molecular diffusion
3	2	5	D_{32}	Sauter mean diameter (SMD)	$\frac{\sum N_i D_i^3}{\sum N_i D_i^2}$	Mass transfer, reaction
4	3	7	D_{43}	De Brouckere or Herdan	$\frac{\sum N_i D_i^4}{\sum N_i D_i^3}$	Combustion equilibrium

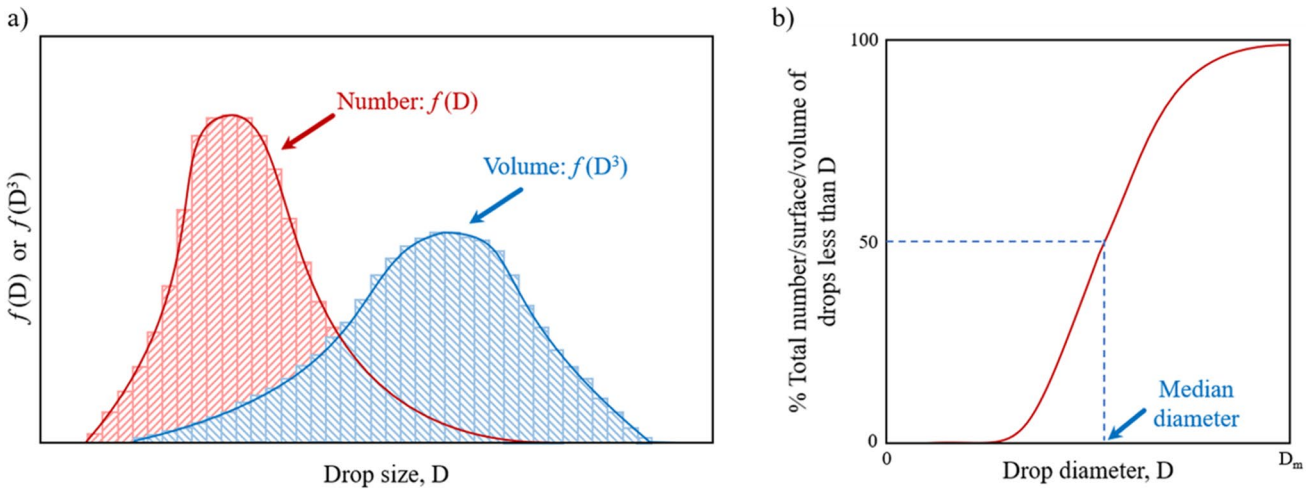

Fig. 4 Drop size distribution: **a** based on number and volume, **b** typical-frequency shape of cumulative curve. Adapted from Lefebvre and McDonell [36]

transfer and flow processes. The concept of mean diameter has been generalized, and its notation was standardized in Eq. (4), where the values of a and b correspond to the effect investigated, the sum a + b is called the order of the mean diameter, i denotes the size range considered, N_i is the number of drops in size range i, and D_i is the middle diameter of size range i. The standard mean diameters definitions are listed in Table 2 [36, 80].

$$D_{ab} = \left[\frac{\sum N_i D_i^a}{\sum N_i D_i^b}\right]^{\frac{1}{a-b}} \tag{4}$$

Alternatively, the Sauter mean diameter and size distribution seem to be the most suitable option for characterizing the droplet cloud. This value is the ratio of the total droplet volume to the total droplet surface. Therefore, it corresponds to the particle diameter with the same volume-to-surface ratio as the entire spray sample. Instead, the median diameter represents the diameter above or below which lies 50% of the number or volume of droplets (Fig. 4). It is especially useful when an excessive amount of very large or very small particles is present [79]. The methodologies and models for estimating droplet size in pneumatic and ultrasonic atomizers are compiled in the following sections.

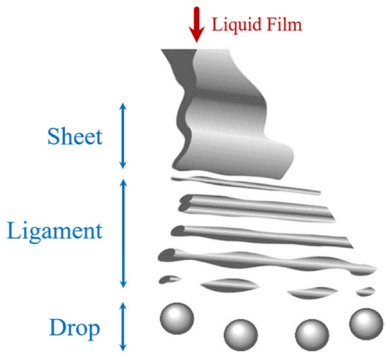

Fig. 5 The two phases of liquid disintegration in pneumatic atomization. Adapted from Schick [60]

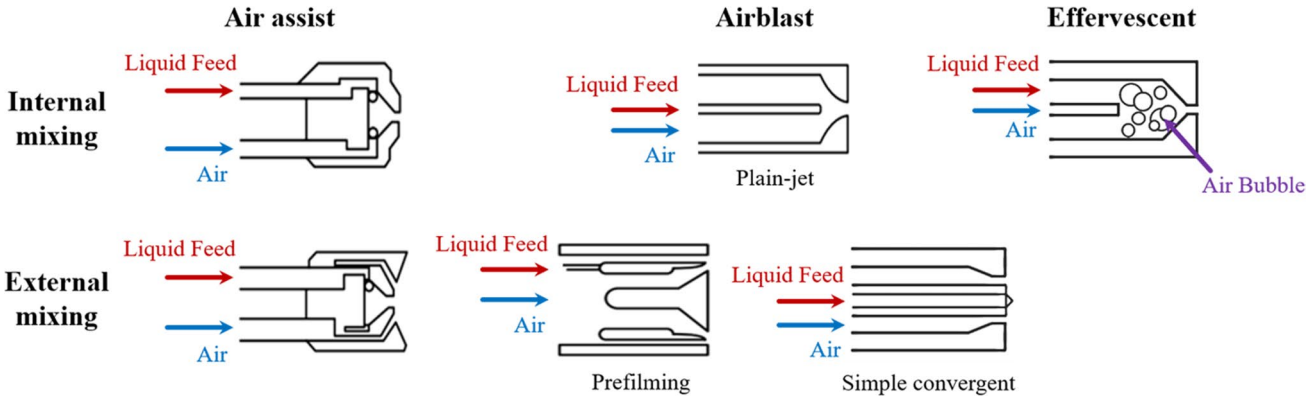

Fig. 6 Twin-fluid atomizers subclassification: air assist, airblast, and effervescent. Adapted from Lefebvre and McDonell [36], Hede et al. [81], and Konstantinov et al. [82]

4.1 Pneumatic atomizer

The pneumatic mechanism of atomization involves high-velocity gas that creates high frictional forces over liquid surfaces, causing a complex situation of liquid instability and a two phases disintegration into spray droplets. The first phase includes the liquid splitting into filaments and large droplets. In contrast, the second completes the atomization by breaking these liquid forms into smaller droplets (Fig. 5). The entire process is influenced by the magnitude of the liquid properties (surface tension, density, and viscosity), and the gaseous flow properties (velocity and density) [60, 81].

In addition to internal or external mixing classification, twin-fluid atomizers can be subclassified into air-assist, airblast, and effervescent atomizers (Fig. 6). The first two employ the kinetic energy of a flowing airstream to splinter the liquid jet or sheet into ligaments and then drops. However, the former uses small quantities of air or steam supplied from a compressor or a high-pressure cylinder flowing at remarkably high velocities (usually sonic), whereas the second employ substantial amounts of air flowing at much lower velocities. Consequently, it is important to keep the airflow rate to a minimum in an air-assist nozzle, and the air velocity through an airblast atomizer is limited to a maximum value (around 120 m/s) [36].

The most usual form of airblast atomizer is the prefilming type (internal or external mixing), in which the liquid is first spread into a thin conical sheet and then exposed to high-velocity airstreams on both sides. Its performance is better than other types of external mixing airblast atomizers, like a simple convergent design. However, pre-filming airblast nozzles are only really effective when both sides of the liquid sheet are exposed to the gas stream. This requirement implies complications in the physical design; therefore, few are being used industrially. Besides, in a plain-jet airblast nozzle (internal mixing), the liquid is injected into the airstream in one or more discrete jets [36, 81].

Otherwise, the atomizing gas is injected into the bulk liquid at low velocity in effervescent atomizers to form a bubbly two-phase mixture upstream of the discharge orifice. Gas bubbles break it into fine fragments and ligaments as the liquid flows through the discharge port. When gas bubbles emerge from the nozzle with a sufficient pressure

drop, they expand so rapidly that the surrounding liquid breaks up into droplets. It is categorized as twin-fluid atomizer with internal mixing [83].

4.1.1 Internal mixing nozzle

Internal mixing nozzles are particularly effective for atomizing highly viscous liquids and liquid slurries. Nevertheless, their aerodynamic and fluid dynamic flow patterns are overly complex because of the intense mixing of gas and liquid within the mixing chamber [36]. The energy difference between the inlet air and emerging spray is the variable that most influences the mean drop size. This effect is described in (Eq. (5), Table 3) for the volume median diameter ($D_{0.5}$ or MMD in μm), where ν_L, $\dot{m}_L$, and σ_L are the kinematic viscosity in cSt, mass flow rate in g/s, and surface tension of the feed liquid in dyne/cm, respectively; ALR is air/liquid mass ratio; ρ_A is the air density in g/cm^3; h is the height of the air annulus in cm; and u_R is the difference between the nozzle atomizing air velocity and the liquid velocity at the nozzle exit in m/s. However, with water spray data, this equation gave an inadequate correlation attributable to the spray's recombination or coalescence of drops. Thus, Eq. (5) should be multiplied by an empirical expression, as shown (Table 3) by Eq. (6), to account for these effects [84]. Additionally, the obtained results through these equations can be converted to SMD (Table 3) with Eq. (7), for an error of ± 5%, as described in Simmons [85]. The empirical formula for SMD in m (Eq. (8)) applies to a range of $\dot{m}_L$ from 30 to 100 kg/h and values of ALR from 0.01 to 0.2, where d_o is the discharge orifice diameter in m (Table 3). The main difficulty of this technique is the mixing of the two phases, so an internal mixing spray can be used to spray high-viscosity liquids and slurries with a wide turn down ratio [36, 86].

The model in Eq. (8) does not incorporate the effect of fluid physical properties such as surface tension, viscosity, or density on the SMD. In order to enhance such estimation, Nath and Satpathy [86] developed an empirical correlation (Eq. (9)) for the prediction of SMD of the spray in terms of various dimensionless groups, like Re (Eq. (10)), Oh (Eq. (11)), and ALR (Table 3). Also, they highlighted the relevance of the investigation and optimization of various process aspects of spray drying of chemical and biological systems, like the temperature and presence/absence of additives, to lead to large savings in labor, cost, and time.

Additional studies on internally mixed air-assist nozzles were carried out by Barreras et al. [87], in which a high-capacity Y-jet configuration was used, and they demonstrated that for a given air mass flow, an increment in water flow increases the air pressure drop; hence the nozzle discharge coefficient is variable depending on the air to liquid ratio. They obtained the correlations for the resulting spray SMD in μm (Table 3) as Eqs. (12)-(14), where ρ_L, u_L, Q_L, and A_{PL} are the density in kg/m^3, initial velocity in m/s, the volumetric flow rate in m^3/h, and total inlet ports area of the feed liquid in m^2, respectively; C is a coefficient representing the efficiency of the atomization process; u_A is the nozzle atomizing air velocity in m/s (average of the measurements in each exit hole using a small Pitot probe without water flow for each air volumetric flow rate); ΔP_L is the injection pressure differential across nozzle in Pa; t is the liquid sheet thickness, which is much less than the outer diameter of the exit holes d_o (both in m); and n_h is the number of holes.

The first studies on a plain-jet airblast atomizer were conducted by Nukiyama and Tanasawa [88]. The drop sizes were measured by collecting spray samples on oil-coated glass slides. Their work with water, alcohol, heavy fuel oil, and gasoline resulted in the empirical formula (Table 3) represented in Eq. (15), where SMD, u_R, σ_L, ρ_L, and μ_L are in μm, m/s, dyne/cm, g/cm^3, dyne·s/cm^2, respectively, and Q_L/Q_A is the ratio of volume flow rate of liquid to volume flow rate of air. This equation is expressed as the sum of two separate terms: the first is dominated by u_R and σ_L and the second by μ_L. Although this correlation is not dimensionally correct, it shows that for liquids of low viscosity, the SMD is inversely proportional to the u_R, while for large values of the air/liquid volumetric flow rate ratio Q_A/Q_L (> 5000), μ_L contributes very little in SMD prediction. Also, as u_R approaches sonic velocity, at a Q_A/Q_L value of 5000 for most nozzles, SMD approaches a constant that depends primarily on ρ_L and σ_L.

Afterward, the performance of plain-jet atomizers was investigated in detail by Lorenzetto and Lefebvre [89], who indicated that the increment of σ_L and μ_L worsens atomization quality and that for low viscosity liquids, SMD is inversely proportional to u_R, and nozzle dimensions have little influence on SMD, conclusions similar to previous works. For high-viscosity liquids, SMD appears to vary in proportion to $d_o^{0.5}$. The expression Eq. (16) for the SMD was derived from an analysis of their experimental data (Table 3). This expression was shown to be accurate to within 8% over the following range properties: μ_L = 0.001–0.076 Pa·s, σ_L = 0.026–0.076 N/m, ρ_L = 79–2180 kg/m^3, u_A = 70–180 m/s, and ALR = 1–16.

Jasuja [90] researched plain-jet atomization using a single nozzle configuration. This investigation evaluated the effects of air and fuel properties on the spray mean drop size characteristics (Eq. (17)) tested for high-viscosity gas oil blends in residual fuel oil (Table 3). The units of this equation are SMD in m, σ_L in N/m, ρ_A, and ρ_L in kg/m^3, u_A in m/s, and μ_L in Pa·s.

Table 3 Drop size equations for internal mixing nozzle

Internal mixing nozzle subclassification	Equations		References
Air assist	$D_{0.5} = 200\nu_L^{0.5}\dot{m}_L^{0.1}\left(1+\frac{1}{ALR}\right)^{0.5}h^{0.1}\sigma_L^{0.2}\rho_A^{-0.3}u_R^{-1.0}$	(5)	[84]
	$D_{0.5} = \left[200\nu_L^{0.5}\dot{m}_L^{0.1}\left(1+\frac{1}{ALR}\right)^{0.5}h^{0.1}\sigma_L^{0.2}\rho_A^{-0.3}u_R^{-1.0}\right]\left[1+2.5\left(\frac{1}{ALR}\right)^{0.6}\dot{m}_L^{0.1}\right]$	(6)	
	$\frac{MMD}{SMD} = 1.2$	(7)	[85]
	$D_{32} = 14E-6\left(\frac{d_o}{ALR}\right)^{0.75}$	(8)	[36, 86]
	$D_{32} = 10.26d_oRe^{-0.869}Oh^{-0.769}ALR^{-0.657}$	(9)	[86]
	$Re = \frac{\rho_L u_R d_o}{\mu_L}$	(10)	
	$Oh = \frac{\mu_L}{\sqrt{\rho_L\sigma_L d_o}}$	(11)	
	$D_{32} = \frac{3}{\frac{1}{t}+\frac{C\rho_L}{4\sigma_L}(u_A^2 ALR+u_L^2)}$	(12)	
	$u_L = \sqrt{\frac{2\Delta P_L}{\rho_L}+\left(\frac{Q_L}{A_{P,L}}\right)^2}$	(13)	[87]
	$t = \frac{Q_L}{\pi n_h d_o u_L}$	(14)	
Plain-jet airblast	$D_{32} = \frac{585}{u_R}\sqrt{\frac{\sigma_L}{\rho_L}}+597\left(\frac{\mu_L}{\sqrt{\sigma_L\rho_L}}\right)^{0.45}\left(\frac{1000Q_L}{Q_A}\right)^{1.5}$	(15)	[88]
	$D_{32} = 0.95\frac{(\sigma_L\dot{m}_L)^{0.33}}{u_R\rho_L^{0.37}\rho_A^{0.30}}\left(1+\frac{1}{ALR}\right)^{1.70}+0.13\mu_L\sqrt{\frac{d_o}{\rho_L\sigma_L}}\left(1+\frac{1}{ALR}\right)^{1.70}$	(16)	[89]
	$D_{32} = 0.022\left(\frac{\sigma_L}{\rho_A u_A^2}\right)^{0.45}\left(1+\frac{1}{ALR}\right)^{0.5}+14.3E-4\left(\frac{\mu_L^2}{\sigma_L\rho_L}\right)^{0.4}\left(1+\frac{1}{ALR}\right)^{0.8}$	(17)	[90]
	$D_{32} = d_0\left[0.48\left(\frac{\sigma_L}{\rho_A u_R^2 d_o}\right)^{0.4}\left(1+\frac{1}{ALR}\right)^{0.4}+0.15\left(\frac{\mu_L^2}{\sigma_L\rho_L d_o}\right)^{0.5}\left(1+\frac{1}{ALR}\right)\right]$	(18)	[91]
	$D_{0.5} = d_o\left(1+\frac{1}{ALR}\right)^{0.28}\left(\frac{\rho_L}{\rho_A}\right)^{0.39}\left[0.010\left(\frac{\sigma_L}{\rho_A u_A^2 d_o}\right)^{0.5}+1.22\left(\frac{\mu_L^2}{\sigma_L\rho_L d_o}\right)^{0.5}\right]$	(19)	[92]
Effervescent	$D_{32} = \frac{12\sigma_L}{\rho_L\left[V_{L1}^2+\varepsilon ALRV_{A1}^2-\frac{(V_{L1}+\varepsilon ALRV_{A1})^2}{1+\varepsilon ALR}\right]}$	(20)	[93]
	$V_{A1} = \sqrt{2RT_n\ln\frac{P_{Ao}}{P_{atm}}}$	(21)	
	$V_{L1} = \sqrt{\frac{2(P_{Lo}-P_{atm})}{\rho_L}}$	(22)	
	$\varepsilon = 1E-4.33(ALR)^{-0.67}$	(23)	[36]
	$\varepsilon = 1E-4.21(ALR)^{-0.56}$	(24)	
	$D_{32} = \left[1.5\sqrt{2}\pi d_l^3\left(1+\frac{3\mu_L}{\sqrt{\rho_L\sigma_L d_l}}\right)\right]^{\frac{1}{3}}$	(25)	[94, 95]
	$D_{32} = 0.00505\left[\left(\frac{ALR}{0.12}\right)^{-0.4686}\left(\frac{\Delta P_L}{5E6}\right)^{-0.1805}\left(\frac{d_o}{0.2}\right)^{0.6675}\left(\frac{\mu_L}{0.2}\right)^{0.1714}\left(\frac{\sigma_L}{46}\right)^{0.1382}\right]$	(26)	[98]
	$D_{32} = \frac{x}{1E4}\left[1.103\left(\frac{ALR}{0.12}\right)^{-0.218}+14.72\left(\frac{ALR}{0.12}\right)^{-0.3952}\left(\frac{\mu_L}{0.2}\right)^{0.1571}\left(\frac{\sigma_L}{46}\right)^{0.8199}\right]$ $+0.00505(1-x)\left[\left(\frac{ALR}{0.12}\right)^{-0.4686}\left(\frac{\Delta P_L}{5E6}\right)^{-0.1805}\left(\frac{d_o}{0.2}\right)^{0.6675}\left(\frac{\mu_L}{0.2}\right)^{0.1714}\left(\frac{\sigma_L}{46}\right)^{0.1382}\right]$	(27)	
	$D_{32} = \frac{x}{1E4}\left[1.103\left(\frac{ALR}{0.12}\right)^{-0.218}\right]+\frac{14.72}{1E4}\left(\frac{ALR}{0.12}\right)^{-0.3952}\left(\frac{\mu_L}{0.2}\right)^{0.1571}\left(\frac{\sigma_L}{46}\right)^{0.8199}$	(28)	

Rizk and Lefebvre [91] have also examined the effects of air and liquid properties and atomizer dimensions on the SMD. They used two geometrically similar atomizers with liquid orifice diameters of 0.55 and 0.75 mm and showed that increases in air pressure P_A, u_A, and ALR ratio tend to lower the SMD. An empirical equation was derived as follows in Eq. (18). Subsequently, Nguyen and Rhodes [92] carried out new experiments to derive the MMD (Eq. (19)), which considers the influence of increased air pressure at high water flows on the drop size through the ratio of the densities of the fluids (Table 3). They found that the size of the mixing chamber did not influence the MMD, and for some test conditions, the MMD was only a weak function of the ALR, contrary to what was mentioned in previous works. This can be because the air–water flow regime experienced in this study is different from previous ones, as well as for high water flows, the required air pressure P_A was higher than for lower water flows with the same air mass flow rate $\dot{m}_A$. This means that the air pressure at the outlet port was greater for high water flow rates, thus dampening the effect on the resulting MMD.

Moreover, Sojka and Lefebvre [93] developed the equations for effervescent atomizer**s** (20)-(22) for computing SMD as a function of ALR associated with the air added to the liquid in the aeration process (Table 3). In these correlations, V_{A1} is the velocity of air at the nozzle exit (isothermal relationship), V_{L1} is the velocity of the liquid at the nozzle exit, R is the ideal gas constant for air, T_n is the initial mixture temperature, P_{Ao} is the pressure of air within the nozzle, P_{atm} is the atmospheric pressure, and P_{Lo} is the pressure of liquid within the nozzle. The empirical constant ε is determined from measured data. As reported by Buckner and Sojka in 1993, glycerin and water mixtures behave as Eq. (23), and glycerin/water/polymer (non-Newtonian) mixtures as Eq. (24) (Table 3). Furthermore, ALRs up to 0.15 provide the most benefit in terms of SMD reduction, highlighting that both Newtonian and non-Newtonian fluid can be effectively atomized using effervescent atomization. For low ALR, the SMD for non-Newtonian liquids is slightly higher. The injection pressure increment has some benefits, but an additional benefit is achieved once a critical minimum pressure is reached [36].

A more fundamental model for the spray SMD (Table 3), where d_l is the ligament diameter, considering the gas and liquid mass flow rates, the liquid physical properties, and the atomizer exit geometry, is described in Eq. (25). This equation neglects the secondary atomization and the aerodynamic effect of the gas surrounding a ligament. However, in effervescent atomization, a significant relative velocity between the gas and the liquid always affects ligament break-up [94, 95]. Therefore, other workers have improved this model by integrating the relative velocity between the gas and ligaments [96] or analyzing the effervescent atomization as a stochastic process that produces a droplet size distribution [97].

Qian et al. [98] provided a more recent expression to calculate SMD for effervescent atomization, which is quite easy to apply as all parameters are well-known and incorporate axial distance from the injector x. Therefore, this correlation is consistent with the notion that the effervescent bubble growth and dynamics are time-dependent due to being farther from the injector, more time has passed, and the effect has more impact on atomization. Equations (26)-(28) describe this relationship for $x \rightarrow 0$, $0 < x < 0.01$ m, and $0.01 < x < 0.2$ m, respectively. The units of this equation are: SMD in m, ΔP_L in Pa, d_o in m, μ_L in Pa·s, and σ_L in N/m (Table 3).

4.1.2 External mixing nozzle

Before a model was established to predict the mean droplet size in air-assist atomizers with external mixing, Simmons [99] presented an equation for the SMD estimation in μm (Eq. (29)) based on data on fuel-pressure-atomizers, airblast nozzles, and air assist simplex nozzles (Table 4). This was done because many of the previous equations do not provide a basis for estimating the effect of dimensions, which is essential in modeling, as well as for achieving a universal or standard approach to cover different nozzle designs. The author considered better developing an estimation methodology for the thickness of a hypothetical film t_F^* instead the film thickness t and used it to facilitate the calculations, development, and compression of his study. It is equivalent to a given volume of fuel flowing at a known axial velocity on the inside of the cylindrical surface of the discharge orifice. In addition, the author made suggestions regarding the choice of constant K_8 for each type of atomizer. Given data for five different air assist simplex nozzles, the recommended value of K_8 for this type of atomizer is 300 and 156 for conventional and SI units, respectively. These values were also recommended for airblast nozzles.

The effect of nozzle geometry, operating variables, and the air pressure on mean drop size, was examined for the atomization of kerosene with 40 different nozzle configurations (Table 4), and the results support Eq. (30) [100]. The dimensionless numbers Re and We of this equation are defined in Eqs. (10) and (31) [36, 100].

The effects of liquid viscosity and surface tension on drop size in an external mixing air-assist atomizer were assessed using various ethanol and glycerin solutions, using a nozzle that produces a liquid flat circular sheet, with thickness ranging from 0 to 0.7 mm by screw rotation [100]. Such a liquid sheet is deflected downward and atomized by an annular air jet, wherein the impingement angle, related to the nozzle axis, can vary. The empirical Eq. (32) fitted the experimental

Table 4 Drop size equations for external mixing nozzle

External mixing nozzle sub-classification	Equations		References
Air assist	$D_{32} = K_8 t_F^{*0.375}\left(\frac{\rho_L^{0.25}\mu_L^{0.06}\sigma_L^{0.375}}{\rho_A^{0.325}}\right)\left(\frac{\dot{m}_L}{\dot{m}_L u_L + \dot{m}_A u_A}\right)^{0.55}$	(29)	[99]
	$D_{32} = 51 d_o Re^{-0.39} We^{-0.18}\left(\frac{1}{ALR}\right)^{0.29}$	(30)	[36, 100]
	$We = \frac{\rho_L d_o u_R^2}{\sigma_L}$	(31)	
	$D_{32} = t\left[1 + \frac{16850 Oh^{0.5}}{We(\rho_L/\rho_A)}\right]\left[1 + \frac{0.065}{ALR^2}\right]$	(32)	[95, 100]
	$Oh = \frac{\mu_L}{\sqrt{\rho_L t \sigma_L}}$	(33)	[36]
	$We = \frac{\rho_A t u_A^2}{\sigma_L}$	(34)	
	$t = \frac{d_o h}{D_{an}}$	(35)	
Prefilming airblast	$\frac{D_{32}}{t} = A\left(\frac{\sqrt{\sigma_L \rho_L}}{\sqrt{t}\rho_A u_A}\right)\left(1 + \frac{1}{ALR}\right) + B\left(\frac{\mu_L^2}{\sigma_L \rho_L t}\right)^{0.425}\left(1 + \frac{1}{ALR}\right)^2$	(36)	[59]
	$D_{32} = A\left(\frac{\sqrt{\sigma_L \rho_L}}{\rho_A u_A}\right)\left(1 + \frac{1}{ALR}\right) + B\left(\frac{\mu_L^2}{\sigma_L \rho_L}\right)^{0.425}\left(1 + \frac{1}{ALR}\right)^2$	(37)	
	$D_{32} = 1E-3\left(\frac{\sqrt{\sigma_L \rho_L}}{\rho_A u_A}\right)\left(1 + \frac{1}{ALR}\right)^{0.5} + 0.6E-4\left(\frac{\mu_L^2}{\sigma_L \rho_L}\right)^{0.425}\left(1 + \frac{1}{ALR}\right)^{0.5}$	(38)	[101]
	$D_{32} = D_h\left(1 + \frac{1}{ALR}\right)\left[0.33\left(\frac{\sigma_L}{\rho_A u_A^2 D_p}\right)^{0.6}\left(\frac{\rho_L}{\rho_A}\right)^{0.1} + 0.068\left(\frac{\mu_L^2}{\sigma_L \rho_L D_p}\right)^{0.5}\right]$	(39)	[102]
	$D_{32} = \frac{3}{\left[\frac{1}{t} + \frac{0.007\rho_L u_A^2}{4\sigma_L\left(1 + \frac{1}{ALR}\right)}\right]}$	(40)	[103, 104]
	$D_{0.5} = d_o\left(1 + \frac{1}{ALR}\right)^{0.45}\left[7.99\left(\frac{\sigma_L}{\rho_A u_A^2 d_o}\right)^{0.87} + 144.6\left(\frac{\mu_L^2}{\sigma_L \rho_L d_o}\right)^{0.87}\right]$	(41)	[92]
Convergent airblast	$D_{0.5} = 2600\left(\frac{\mu_A}{ALR \rho_A u_A L}\right)^{0.4}$	(42)	[105]
	$D_{0.5} = 249\left[\frac{\sigma_L^{0.41}\mu_L^{0.32}}{(u_R^2 \rho_A)^{0.57} A^{0.36} \rho_L^{0.16}}\right] + 1260\left(\frac{\mu_L^2}{\rho_L \sigma_L}\right)^{0.17}\frac{ALR^m}{u_R^{0.54}}$	(43)	[106]
	$D_{32} = 9.503\left(\frac{ALR}{ALR_{ref}}\right)\exp(0.7158 d_o)$	(44)	[107]
	$D_{0.5} = 7.398\left(\frac{ALR}{ALR_{ref}}\right)\exp(0.7235 d_o)$	(45)	

data, where d_o is the outer diameter of pressure nozzle (Table 4), t is the initial film thickness, D_{an} is the diameter of the annular gas nozzle, and h is the slot width of the pressure nozzle. The dimensionless numbers Oh and We, as well as the t value of Eq. (32), are defined in Eqs. (33)-(35), respectively [36, 95, 100].

In contrast, both internal and external mixing airblast nozzles can be used as prefilming atomizers; however, droplet size in prefilming airblast atomizers with external mixing has been analyzed and reported more frequently and in-depth. Rizkalla [84] studied the performance of a prefilming airblast atomizer, wherein the liquid is first spread into a thin sheet, then exposed to high-velocity air streams on both sides. One year later, Rizkalla and Lefebvre [59] suggested a form of dimensionless relationship (Eq. (36)) wherein the SMD is reported as the summation of two terms: the first governed by air momentum and surface tension, and the second ruled by liquid viscosity (Table 4). The first term prevails for liquids of low viscosity, where the SMD increases with the rise of σ_L, ρ_L, and prefilmer diameter D_p and decreases with increases in u_A, ALR, and ρ_A. On the other hand, in high-viscosity liquids, the second term gets greater significance, and the SMD becomes less sensitive to variations in u_A and ρ_A.

Nevertheless, the dimensionless constants A and B in Eq. (36) cannot be estimated, due to the lack of experimental data on the thickness of liquid film (t) at the prefilming lip. As a result, Eq. (36) might be modified as in Eq. (37) for SI units (Table 4), neglecting the term related to the film thickness. Although this equation was developed for the specific atomizer used in their study, it may be helpful in other prefilming airblast atomizers. If drop size data are available. The

constants A and B can be fitted to the experimental data. In this work, A = 6.5E-4 and B = 1.2E-4. This expression demonstrated to be precise over the following properties ranges: μ_L = 0.001–0.044 Pa·s, σ_L = 0.026–0.074 N/m, ρ_L = 780–1500 kg/m^3, u_A = 70–125 m/s, and ALR = 2–6 [59].

Equation (38) by Jasuja [101] is very similar to Eq. (37). They have the same layout of the equation, but the difference is in the exponent of the factors with ALR (Table 4). This change was made to diminish the predicted effect of the second term (viscosity) in Eq. (37) and thereby redress the relative contribution of the two terms.

El-Shanawany and Lefebvre [102] evaluated the effect of the linear atomizer scale on the mean drop size using three comparable external mixing prefilming airblast atomizers. They considered cross- sectional areas in the ratio of 1:4:16 and with prefilmer lip diameters of 19.05, 38.10, and 76.20 mm. They found that spray quality declines with an increase in atomizer size. A dimensionally correct Eq. (39) for relating the experimental data on SMD to the flow variables and atomizer dimensions was derived, wherein D_h represents the hydraulic mean diameter of the air exit channel (Table 4).

Given the difference in atomization mechanisms for external mixing prefilming airblast, Lefebvre [103] suggests the dimensionally correct Eq. (40) for prompt atomization (Table 4). The value of 0.007 was derived from the best data fit from Beck et al. [104], and it is a function of the impingement angle of the air on the liquid sheet. Most likely, that value would increase as the angle increases.

Additionally, Nguyen and Rhodes [92] suggested a modified version of Eq. (19), for a novel prefilming external mixing nozzle able to produce very fine droplets at low ALR, as described in Eq. (41). This change was proposed considering that in the prefilming atomization, only air flows through the nozzle (Table 4). Therefore, the air pressure at the nozzle only depends on the air mass flow rate, being constant regardless of the water flow rate, showing a stronger dependence on ALR compared to the internal mixing type of atomization.

Finally, for other types of external mixing airblast with a simple design, Gretzinger and Marshall [105] evaluated the mean droplet size and droplet size distribution for a converging nozzle in which the liquid is first brought into contact with the atomizing airstream at the throat of an air nozzle. Their experiments covered liquid flow rates from 2 to 17 L/h, utilizing liquid orifice diameters of 2.4, 2.8, and 3.2 mm. Their experimental results were correlated by Eq. (42) in the drop diameters range from 5 to 30 µm, where SMD is in µm, L is a specific nozzle length, equivalent to the wetted boundary between the air and liquid streams, regularly estimated by the d_o, and μ_A is the air viscosity (Table 4).

Kim and Marshall [106] also evaluated a convergent external mixing nozzle, similar to that used by Gretzinger and Marshall [105]. They measured droplet size on melts of wax mixtures, with μ_L ranging from 0.001 to 0.050 Pa·s, u_R from 75 to 393 m/s, ALR of 0.06 to 40, ρ_L of 800 to 960 kg/m^3, and ρ_A of 0.93 to 2.4 kg/m^3. The empirical Eq. (43) was obtained by fitting the experimental data, where m = −1 at ALR < 3, m = −0.5 at ALR > 3, and A is the area of the air annulus in ft^2 (Table 4). The units of this equation are: SMD in µm, σ_L in dyne/cm, μ_L in cP, u_R in ft/s, and ρ_A and ρ_L in lb/ft^3.

Other works, such as that of Sander and Penović [107], used Kim and Marshall's research [106] and proposed a simple method for predicting droplet size distribution from a reference particle size distribution. Experiments were conducted on a laboratory-scale spray dryer (Mini Spray Dryer, Buchi 290) equipped with a dehumidifier. For atomization, two-fluid nozzles (external mixing) of different inner diameters (0.7, 1.4, and 2.0 mm) were employed. Various mean droplet sizes in µm were correlated with the ALR and d_o (Eqs. (44)-(45) in Table 4, where ALR_{ref} is the ALR of the reference material, in this case, bismuth molybdate suspension). The method was tested with powders obtained by spray drying a suspension of glycine particles in a saturated aqueous solution and suspensions of microcrystalline cellulose in aqueous solutions of PVP. The proposed methodology can be applied when non-agglomerated particles, spherical particles, or spherical agglomerates are obtained by spray drying. The droplet size and distribution are influenced by the suspension properties like surface tension and viscosity, nozzle diameter, and air/suspension mass flow ratio for the investigated systems.

5 Theory of ultrasound atomization. Models for estimation of droplet size

Wood and Loomis [108] were the first ones to use ultrasound to obtain a fog formation, while Söllner [109] investigated and reported the mechanism of atomization, concluding that cavitation plays a significant role in this phenomenon. The ultrasonic atomization has been explained by two hypotheses: cavitation theory and capillary wave theory. The first indicates that droplet formation is controlled by cavitation, which is the formation of the cavity in the liquid film on the vibrating surface of an atomizer. Cavities are repeatedly expanded, contracted, and eventually collapse. Fine droplets are ejected from the liquid surface by the shock waves generated by cavity collapse. Cavitation occurs randomly, introducing random variations in the mist size. In contrast, the second theory considers the formation of capillary waves composed of crests and troughs on the vibrating surface. Therefore, the droplet size of the generated mist depends on the wavelength

of the capillary waves: if the capillary wavelength decreases, the frequency of the ultrasonic waves increases, and finer mist is generated [3, 110]. Kelvin's equation [111] used for determining the wavelength of capillary waves λ is as follows, where f is the ultrasonic frequency:

$$\lambda = \left(\frac{8\pi\sigma}{\rho f^2}\right)^{\frac{1}{3}} \tag{46}$$

Experimental data can be used to correlate the capillary wavelength with the number/volume-median and most probable size of ultrasonic atomized particles, and usually, it is a constant fraction of the capillary wavelength (Eq. (47)) [9]. Lang [112] was one of the first researchers to determine a correlation for an ultrasonic nozzle. The author predicted the number-median diameter of the droplets generated (Eq. (39) with a = 0.34) from the crests of capillary waves for different working fluids, including water, oil, and molten waxes at forced vibration frequencies of 10–800 kHz. This relation is in close agreement with Lobdell's theoretical value of a = 0.36 [113] for the most probable size of the particle, a result obtained from considerations of drop formation from high amplitude capillary waves. For MHz-range ultrasound, the constant a was modified to 0.96 by Yasuda et al. [114] for volume-median droplet diameter of aqueous alcohol solution, which was observed with the laser diffraction method.

$$d_p = a\lambda = a\left(\frac{8\pi\sigma}{\rho f^2}\right)^{\frac{1}{3}} \tag{47}$$

Peskin and Raco [115] also assumed that the droplet size is proportional to the wavelength of capillary waves resulting from consideration of the unstable forced motion of a liquid film (Eq. (48)). Instead, Dobre and Bolle [116] used this proportion to establish an estimation of the mean volume diameter (Eq. (49)).

$$d_p = \left(\frac{4\pi^3\sigma}{\rho f^2}\right)^{\frac{1}{3}} \tag{48}$$

$$D_{30} = 0.73\left(\frac{\sigma}{\rho f^2}\right)^{\frac{1}{3}} \tag{49}$$

Data obtained from an ultrasonic atomizer, operating at a frequency of 26 kHz, at flow rates Q up to 50 L/h, and using distilled water and solutions of water with methanol and glycerin, was used to support Eq. (50) for SMD in m (σ is in kg/s^2, ρ is in kg/m^3, μ is in kg/m·s, and Q is in m^3/s). This analysis evaluated the influence of suitable variations in the atomization liquid properties [36, 95]. However, this correlation ignores the frequency and amplitude oscillation parameters and could deliver inadequate results [9].

$$D_{32} = 0.158\left(\frac{\sigma}{\rho}\right)^{0.354}\mu^{0.303}Q^{0.139} \tag{50}$$

Hence, Rajan and Pandit [117] proposed a unified correlation that accounted for all the relevant physicochemical properties of the feed liquid and the ultrasonic atomizer characteristics (Eq. (51)). This equation uses modified dimensionless numbers We and Oh to consider the frequency of irradiation, as well as proposes a dimensionless number called Intensity number (In) to contemplate the effect of ultrasonic intensity (Eqs. (52)-(54)). Thus, the concept of critical Weber, where inertial and surface tension forces are equilibrated, that is $We_c = 1$, was extended to ultrasonic atomization and defined the critical flow rate Q_c (Eq. (55)) as the threshold above which the flow rate influences the size of the droplets. Then, the maximum flow rate, above which dripping forms larger droplets, is considered. Then, the maximum flow rate is the volumetric displacement rate of the vibrating surface, given by the product of frequency f, the amplitude of sound wave A_m, and the area of vibrating surface A. If this liquid flow is exceeded, dripping due to gravity takes place, and larger drops are formed. The amplitude is defined as the Eq. (56), where I is the power surface intensity (the ratio between the power delivered at the surface P, and the vibrating surface area) and C is the sound speed in the liquid medium. Also, the threshold amplitude for capillary waves (A_{mc}) to break into droplets for spray formation was given in Eq. (57).

$$d_p = \left(\frac{\pi\sigma}{\rho f^2}\right)^{0.33}[1 + 0.1(We)^{0.22}(Oh)^{0.166}(In)^{-0.0277}] \quad (51)$$

$$We = \frac{fQ\rho}{\sigma} \quad (52)$$

$$Oh = \frac{\mu}{fA_m^2\rho} \quad (53)$$

$$In = \frac{f^2A_m^4}{CQ} \quad (54)$$

$$Q_c = \frac{\sigma}{f\rho} \quad (55)$$

$$A_m = \frac{1}{2\pi f}\sqrt{\frac{2I}{\rho C}} \quad (56)$$

$$A_{mc} = \left(\frac{2\mu}{\rho}\right)\left(\frac{\rho}{\sigma f\pi}\right)^{\frac{1}{3}} \quad (57)$$

Avvaru et al. [118] included the atomizing liquid's rheological, pseudoplastic nature (non-Newtonian behavior). They obtained a correlation for an aqueous carboxymethylcellulose solution with a shear-thinning behavior and a flow behavior index n (Eq. (50)). Barba et al. [119] proposed a modification of Eq. (58), tested during the ultrasonic atomization of alginate solutions (Eq. (59)). To understand the effect of frequency on droplet size distribution, Ramisetty et al. [3] evaluated three different ultrasonic atomizers operating at frequencies of 20, 40, and 130 kHz, respectively. They developed the Eq. (60) applicable in the following ranges: f = 20–130 kHz, ρ = 912–1151 kg/m^3, σ = 0.0029–0.073 N/m, Oh = 2.71–161.64, We = 14.8–571, and In = 3.65E − 13–1.92E − 9. In these three equations, d_p is in m, σ is in kg/s^2, ρ is in kg/m^3, and f is in Hz.

$$d_p = \left(\frac{\pi\sigma}{\rho f^2}\right)^{\frac{1}{3}} + 0.0013(We)^{0.008}(Oh)^{-0.14/n}(In)^{0.28} \quad (58)$$

$$d_p = 0.058\left(\frac{\pi\sigma}{\rho f^2}\right)^{0.33}(We)^{0.151}(Oh)^{0.192}(In)^{-0.02} \quad (59)$$

$$d_p = 0.00154\left(\frac{\pi\sigma}{\rho f^2}\right)^{0.33}[1 + \left(\frac{\pi\sigma}{\rho f^2}\right)^{-0.2}(We)^{0.154}(Oh)^{-0.111}(In)^{-0.033}] \quad (60)$$

Through all the studies on ultrasonic atomization developed so far, it can be concluded that the operation characteristics and atomizer geometry can control the phenomena of cavitation and capillary wave. Overall, the size of the drop is a function of the liquid's properties and equipment's characteristics and operation.

6 Evaluation of different factors influencing droplet size in pneumatic and ultrasonic atomization

This section discusses the effect of the properties of the atomized liquid, characteristics of the atomizer, and operating conditions on the droplet size for both pneumatic and ultrasonic atomizers. Selected models previously introduced were used to calculate the droplet size per different study cases. All calculations, experimental data recovery, and sensitivity

analysis plots were performed in MATLAB® R2020b. For the internal and external mixing pneumatic atomization, the effect of μ_L, σ_L, ρ_L, u_A, and ALR is studied. The parameters proposed for the internal mixing nozzle were based on Lorenzetto and Lefebvre [89], while for the external mixing nozzle the reported data by Rizkalla [84] and Rizkalla and Lefebvre [59] were used. Equations (16) and (37) were used to study internal and external atomization, respectively. Otherwise, for ultrasonic atomization, the effect of f, P, μ_L, σ_L, and Q is analyzed. In this case, Eq. (51) by Rajan and Pandit [117] and Eq. (60) by Ramisetty et al. [3] were implemented to evaluate the different estimations. The proposed parameters were based on Ramisetty et al. [3], except for C values, which are reported by Lide [120]. For A values, A_m was fitted to Eq. (60) with the experimental data of Ramisetty et al. [3], considering that the equation fits better with Oh = 2.71–161.64. Subsequently, the value of A was calculated by solving Eq. (56).

Figures 7 and 8 display the sensitivity analysis for both types of pneumatic atomizers, internal and external respectively. As can be observed, droplet size decreases with increasing air-to-liquid ratio (ALR). At low ALR, the amount of atomizing air is insufficient to overcome the viscous and surface tension forces, which act together to oppose drop formation, therefore, the droplet size is larger; at ALR values greater than or equal to 4, there is no significant change in droplet size. To improve the quality of atomization the liquid has to be exposed to the highest possible air velocity [36, 81].

Regarding the feed liquid viscosity the droplet size increases with the increment this variable (Figs. 7a and 8a). This is usually attributed to viscous forces, which tend to oppose the disintegration of liquids into droplets and resist any further break-up of already-formed droplets [84, 89]. Other effects of increasing viscosity are decreased liquid flow rate, higher minimum pressure requirement to maintain proper spray angle/coverage, and increased volume of liquid at a given SMD and distribution produced per unit of time [81]. Similarly, the droplet size increases with the increment of the feed liquid surface tension (Figs. 7b and 8b), due to this liquid property opposes any distortion or irregularity in the liquid surface, delaying the start of ligament formation. Additional effects of increasing surface tension are increased minimum operating pressure and decreasing spray angle [81, 84].

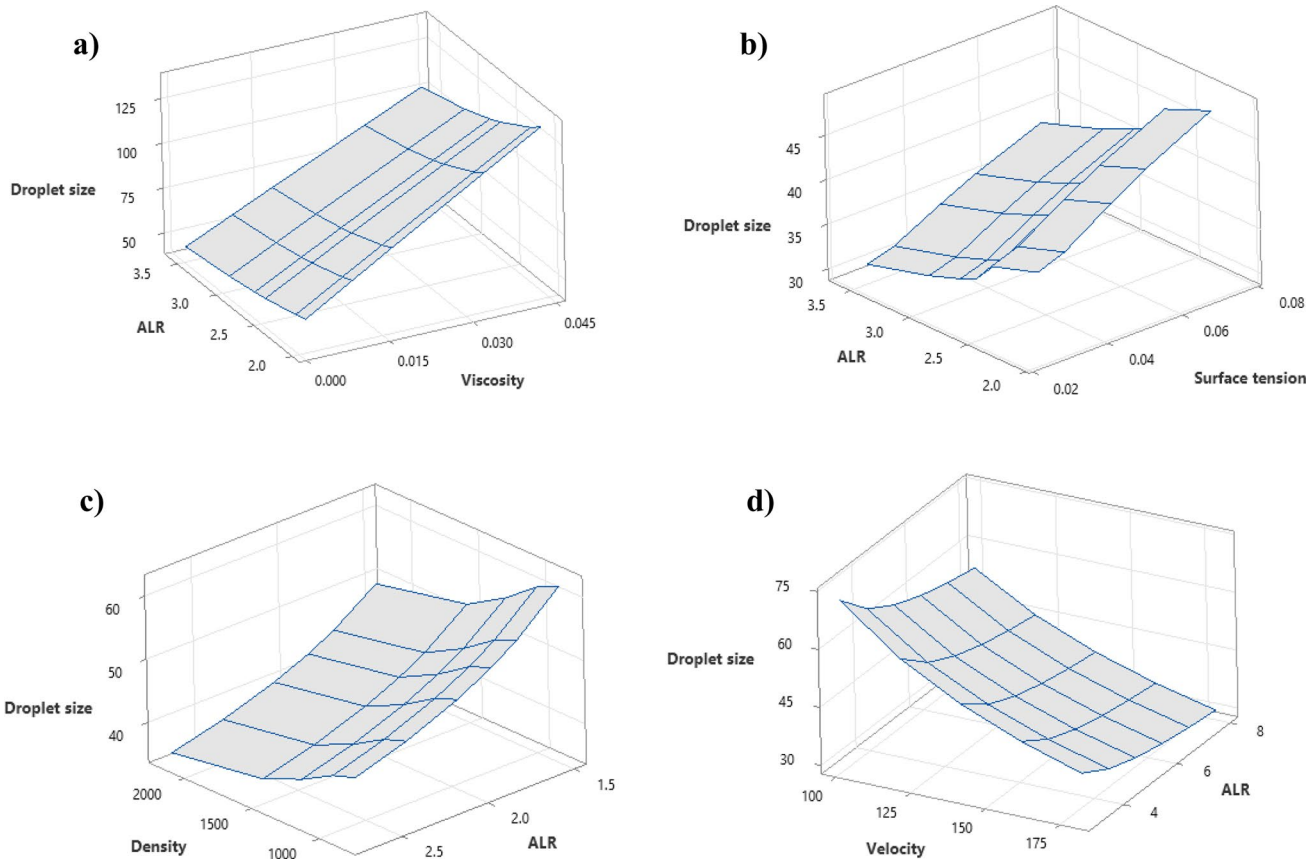

Fig. 7 Sensitivity analysis for droplet size (SMD) given the case studies of the internal mixing pneumatic atomizer: **a** viscosity (μ_L, [Pa·s]) and ALR, **b** surface tension (σ_L, [N/m]) and ALR, **c** density (ρ_L, [(kg/m^3]) and ALR, **d** air velocity (u_R, [m/s]) and ALR

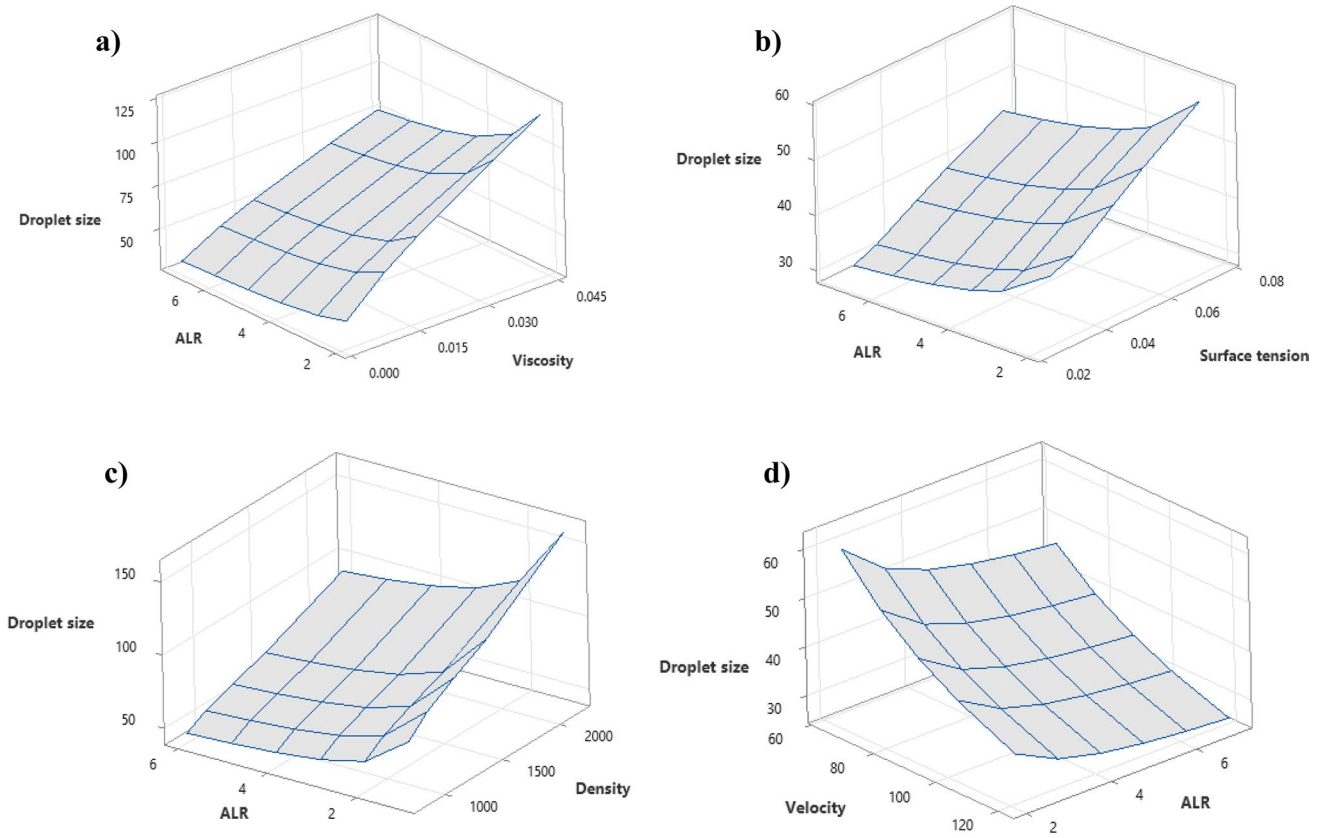

Fig. 8 Sensitivity analysis for droplet size (SMD) given the case studies of the external mixing pneumatic atomizer **a** viscosity (μ_L, [Pa·s]) and ALR, **b** surface tension (σ_L, [N/m]) and ALR, **c** density (ρ_L, [(kg/m^3]) and ALR, **d** air velocity (u_A, [m/s]) and ALR

On the other hand, the effect of liquid density is different between the two types of pneumatic atomizers. Figure 7c shows an increase in droplet size with decreasing density, while Fig. 8c shows an inverse effect.

This phenomenon is due to a competition of factors related to the mechanism and shape of the pneumatic atomizer. In the external mixing prefilming atomizers, the distance at which the coherent fluid sheet extends down the atomizing edge increases with density, so that ligament formation occurs in conditions of the lower relative speed between air and liquid; as well as an increase in liquid density produces a more compact spray that is less exposed to high-speed air atomization action [36, 81]. Therefore, the effect of liquid density is complex, but in general, a more effective atomization process (smaller droplet size) is demonstrated in plain-jet internal mixing nozzles than in prefilming external mixing nozzles by increasing the density of the liquid.

As shown in Figs. 7d and 8d, the droplet size decreases with the increase in air velocity (u_R for internal mixing nozzle cases is considered very close to u_A as previously mentioned). This is due to the principle of operation of pneumatic atomizers, which use the kinetic energy of a flowing air current to break the jet or sheet of liquid into ligaments and then in drops; to improve the quality of atomization the liquid needs to be exposed to the highest possible air velocity [36, 81].

For the ultrasonic atomization, Figs. 9 and 10 show the sensitivity analyses using Eq. (51) by Rajan and Pandit [117] and Eq. (60) by Ramisetty et al. [3], respectively. The estimations with the first equation tend to be lower than the second, a behavior also pointed out by Ramisetty et al. [3]. Overall results show that droplet size increases with increasing liquid flow rate since an increase in the thickness of the liquid film formed on the vibrating surface before atomization. Below a critical flow rate Q_c, the liquid cannot cover the entire atomization surface, so no effective atomization occurs. Above Q_c, the droplet size is proportional to the liquid flow rate. With higher flow rate increments, it results in lower cavitation near the film surface, forming large droplets with a higher size distribution, as cavitation influences capillary waves randomly or, in certain cases dripping of liquid may occur [2, 3, 9].

Figures 9a and 10a show that as the frequency decreases, the droplet size increases. Increasing the frequency results in a lower wavelength, and therefore the atomizing liquid undergoes a large number of compression cycles, reducing

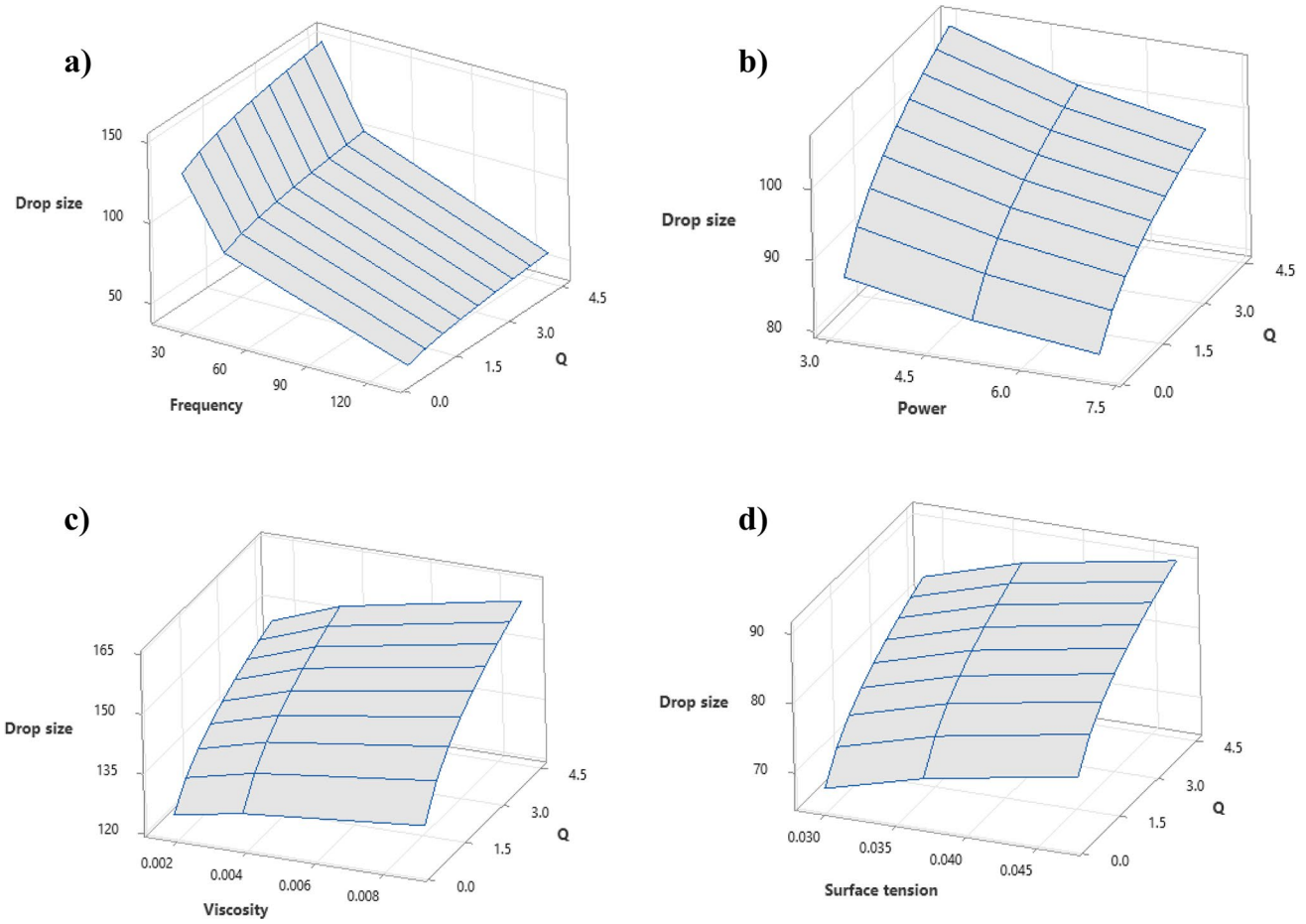

Fig. 9 Sensitivity analysis for droplet size (SMD) given the case studies of the ultrasonic atomizer and using Eq. (51) by Rajan and Pandit [117]: **a** Frequency (f [kHz]) and flowrate (Qx10^7, [m^3/s]), **b** Power (P, [W]) and flowrate (Qx10^7, [m^3/s]), **c** Viscosity (μ_L, [Pa·s]) and flowrate (Qx10^7, [m^3/s]), **d** Surface Tension (σ_L, [N/m]) and flowrate (Qx10^7, [m^3/s])

the size of the droplets; increasing frequency also induces an increase in the droplet ejection rate, as well as a decrease in the peak diameter in the drop size frequency distribution curve [110, 121, 122].

The effect of increasing power shows a different behavior depending on the selected equation; Fig. 9b indicates a decrease in droplet size, while Fig. 10b illustrates the opposite. This discrepancy had already been observed by Avvaru et al. [118], who coincide with the results of Ramisetty et al. [3]. They explain that an increase in power is related to the vibratory amplitude A_m, which is proportional to the intensity I, and therefore, to the power P. With the increase of A_m, a greater height of the capillary waves is obtained, and the volume of the atomization liquid increases, leading to a larger droplet size [9].

As the power, the effect of the liquid viscosity presents differences between the results obtained by the two approaches (Figs. 9c and 10c). With Eq. (51), droplet size increases with the increase in viscosity, and Eq. (60) shows the opposite behavior. Also, Avvaru et al. [118] differed from Rajan and Pandit [117] and got behaviors similar to Ramisetty et al. [3]. As the liquid viscosity increases, the liquid cannot be atomized immediately when it leaves the nozzle orifice, so the residence time of the liquid on the atomizing surface increases, and its temperature also increases due to the dissipation of vibrational energy. The change in temperature causes the viscosity of the liquid to decrease to a critical value, and a smaller droplet size is obtained. Additionally, in fluids with low viscosity, the hydraulic shock produced during cavity collapse can tear larger volumes of liquid from the liquid film due to less damping of the propagating shock wave, so the droplet size is larger.

In contrast, in high-viscosity fluids, the intensity of the hydraulic shock produced is very low, because the sound waves (pressure) coming from the oscillating surface are quickly damped as they are unable to overcome the cohesive forces

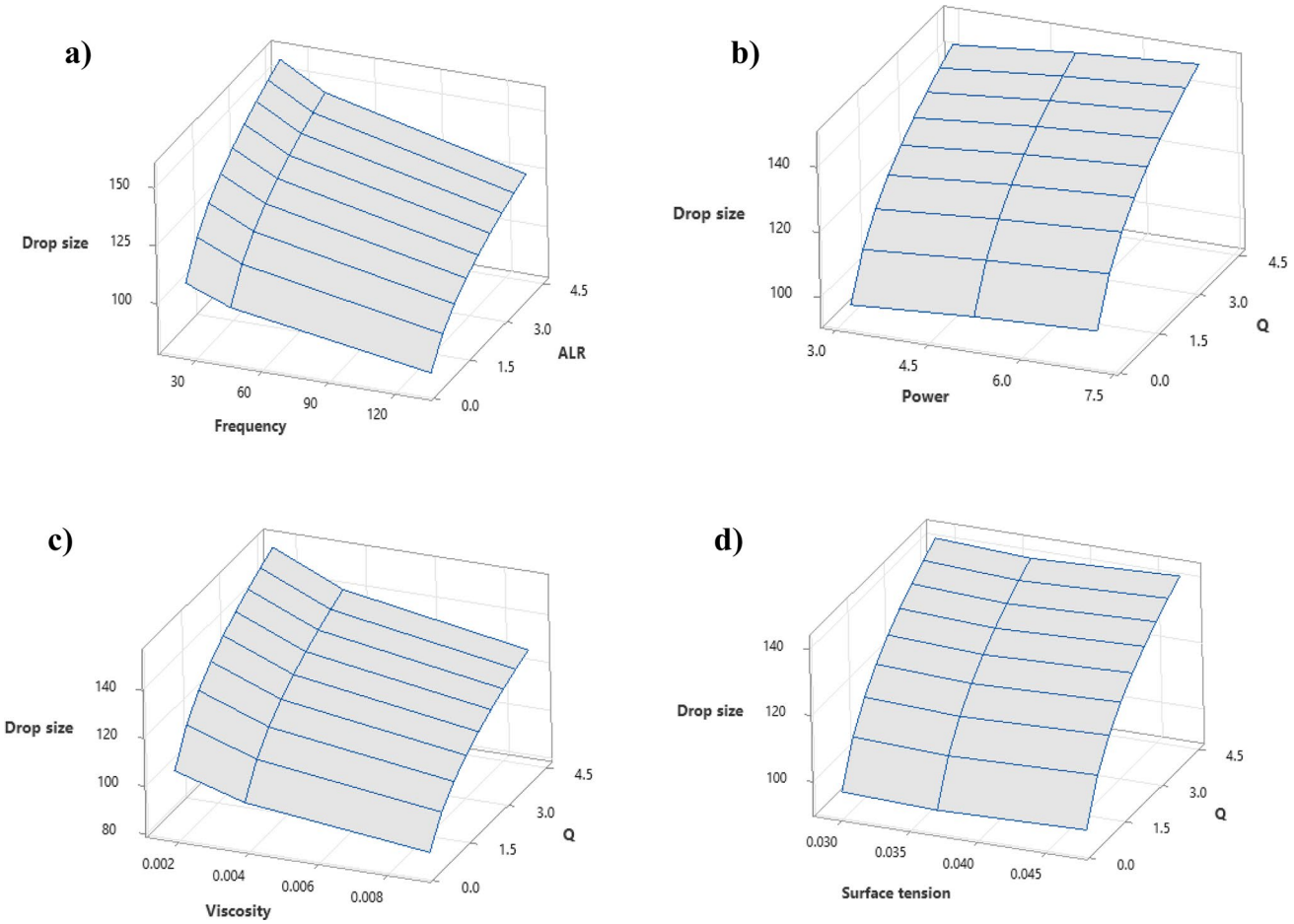

Fig. 10 Sensitivity analysis for droplet size (SMD) given the case studies of the ultrasonic atomizer and using Eq. (60) by Ramisetty et al. [3]: **a** Frequency (f [kHz]) and flowrate (Qx10^7, [m^3/s]), **b** Power (P, [W]) and flowrate (Qx10^7, [m^3/s]), **c** Viscosity (μ_L, [Pa s]) and flowrate (Qx10^7, [m^3/s]), **d** Surface Tension (σ_L, [N/m]) and flowrate (Qx10^7, [m^3/s])

between the liquid molecules, therefore that only those cavitation bubbles that are closer to the gas/liquid film, when collapsing, can remove a tiny volume of the liquid from the surface, generating a smaller droplet size [118].

Finally, results show a decrease in droplet size with decreasing surface tension (Figs. 9d and 10d). However, these variations are minimal between the three values of surface tension. Ramisetty et al. [3] and Dalmoro et al. [2] explain that when the surface tension decreases, the number of capillary waves per unit vibratory area increases at higher amplitudes, causing immediate droplet ejection from the crests and a corresponding decrease in droplet size, but that eject at high speeds.

7 Final remarks

Some atomization applications in the food industry have been presented, highlighting the importance of droplet size, which determines the effectiveness of spraying for some established purposes of operational design, quality food properties, safety, and economics. The development of atomization theory has been presented in this review, illustrating the implementation of selected models for pneumatic and ultrasonic atomization. The effect of the atomized liquid's properties, the atomizer's characteristics, and the operating conditions on the droplet size is discussed. When studying the effect of air/liquid mass ratio, air velocity, viscosity, surface tension, and density of the atomized liquid in internal and external mixing type pneumatic atomizers, similar conclusions are obtained with the first four factors and the last variable differs depending on the mechanism and geometry of the atomizer. Otherwise, the effect

of flow rate, frequency, power, viscosity, and surface tension was discussed in ultrasonic atomization. The droplet size increases with the increase in flow rate, power, and surface tension, while it decreases with the increase in viscosity and frequency, where these last two variables, together with the flow rate, are the most influential factors in this type of atomization. This work has summarized and selectively presented the expressions that best predict droplet size under specific system parameters, outlining their advantages and limitations. As described, atomization has acquired a rising interest in the food industry, so this work intends to provide the reader with a valuable reference for future research for analyzing the expected behavior and fineness of an atomization process for different applications in food processing.

Author contributions Mariola Camacho-Lie wrote de original draft and prepare the figures. Oscar Antonio-Gutiérrez and Andrea Selene López-Díaz wrote and edited the main manuscript. Aurelio López-Malo reviewed and edited the main manuscript. Nelly Ramírez-Corona conceptualized, supervised, and edited the main manuscript.

Funding No funding was received to assist with the preparation of this manuscript.

Data availability The authors confirm that the data supporting the findings of this study are available within the article.

Code availability Not applicable.

Declarations

Competing interests The authors have no competing interests to declare that are relevant to the content of this article.

References

1. Rozali SNM, Paterson AHJ, Hindmarsh JP, Huffman LM. Theoretical prediction of atomization performance of fibre suspensions and the effect of feed temperature and air velocity. J Food Eng. 2020;269: 109742. https://doi.org/10.1016/j.jfoodeng.2019.109742.
2. Dalmoro A, Barba AA, d'Amore M. Analysis of size correlations for microdroplets produced by ultrasonic atomization. Sci World J. 2013;2013:1–7. https://doi.org/10.1155/2013/482910.
3. Ramisetty KA, Pandit AB, Gogate PR. Investigations into ultrasound induced atomization. Ultrason Sonochem. 2013;20(1):254–64. https://doi.org/10.1016/j.ultsonch.2012.05.001.
4. Zhao H, Liu H. Breakup morphology and mechanisms of liquid atomization. In: Agarwal RK, editor. Environmental impact of aviation and sustainable solutions. London: IntechOpen; 2019. https://doi.org/10.5772/intechopen.84998.
5. Movahednejad E, Tabatabaei A, Ranjbaran AR. Developing a model to predict droplet size and velocity distribution of a liquid fuel swirl nozzle spray. In: Asian Congress on Gas Turbines 2012; 2012.
6. Samborska K, Poozesh S, Barańska A, Sobulska M, Jedlińska A, Arpagaus C, Malekjani N, Jafari SM. Innovations in spray drying process for food and pharma industries. J Food Eng. 2022;321:110960. https://doi.org/10.1016/j.jfoodeng.2022.110960.
7. Gogate PR. 30—The use of ultrasonic atomization for encapsulation and other processes in food and pharmaceutical manufacturing. In: Gallego-Juárez JA, Graff KF, editors. Power ultrasonics: applications of high-intensity ultrasound. Sawston: Woodhead Publishing; 2015. https://doi.org/10.1016/B978-1-78242-028-6.00030-2.
8. Zhang ZH, Wang LH, Zeng XA, Han Z, Brennan CS. Non-thermal technologies and its current and future application in the food industry: a review. Int J Food Sci Technol. 2018;54(1):1–13. https://doi.org/10.1111/ijfs.13903.
9. Khaire RA, Gogate PR. Novel approaches based on ultrasound for spray drying of food and bioactive compounds. Dry Technol. 2020;39(12):1832–53. https://doi.org/10.1080/07373937.2020.1804926.
10. O'Sullivan JJ, Norwood EA, O'Mahony JA, Kelly AL. Atomisation technologies used in spray drying in the dairy industry: a review. J Food Eng. 2019;243:57–69. https://doi.org/10.1016/j.jfoodeng.2018.08.027.
11. Candia-Muñoz N, Ramirez-Bunster M, Vargas-Hernández Y, Gaete-Garretón L. Ultrasonic spray drying vs high vacuum and microwaves technology for blueberries. Phys Procedia. 2015;70:867–71. https://doi.org/10.1016/j.phpro.2015.08.178.
12. Izidoro DR, Sierakowski MR, Haminiuk CWI, de Souza CF, de Scheer AP. Physical and chemical properties of ultrasonically, spray-dried green banana (Musa cavendish) starch. J Food Eng. 2011;104(4):639–48.
13. Antonio-Gutiérrez O, López-Malo A, Ramírez-Corona N, Palou E. Enhancement of UVC-light treatment of tangerine and grapefruit juices through ultrasonic atomization. Innov Food Sci Emerg Technol. 2017;39:7–12. https://doi.org/10.1016/j.ifset.2016.10.019.

14. Semyonov D, Ramon O, Shimoni E. Using ultrasonic vacuum spray dryer to produce highly viable dry probiotics. LWT - Food Sci Technol. 2011;44(9):1844–52. https://doi.org/10.1016/j.lwt.2011.03.021.
15. Jiang M, Bai X, Sun J, Zhu W. Implication of ultrasonic power and frequency for the ultrasonic vacuum drying of honey. Dry Technol. 2021;39(10):1389–400. https://doi.org/10.1080/07373937.2020.1750026.
16. Isleroglu H, Turker I, Koc B, Tokatli M. Microencapsulation of microbial transglutaminase by ultrasonic spray-freeze drying. Food Bioprocess Technol. 2019;12(12):2004–17. https://doi.org/10.1007/s11947-019-02353-4.
17. Bravin B, Peressini D, Sensidoni A. Development and application of polysaccharide–lipid edible coating to extend shelf-life of dry bakery products. J Food Eng. 2006;76(3):280–90. https://doi.org/10.1016/j.jfoodeng.2005.05.021.
18. Chopde S, Datir R, Deshmukh G, Dhotre A, Patil M. Nanoparticle formation by nanospray drying and its application in nanoencapsulation of food bioactive ingredients. J Agric Food Res. 2020;2: 100085. https://doi.org/10.1016/j.jafr.2020.100085.
19. Vickovic D, Pedersen SJ, Ahrné L, Hougaard AB. Effects of lactic acid concentration and spray drying conditions on stickiness of acidified skim milk powder. Int J Dairy Technol. 2023;76(2):266–75. https://doi.org/10.1111/1471-0307.12932.
20. Berk Z. Dehydration. In: Berk Z, editor. Food process engineering and technology food science and technology. Cambridge: Academic Press; 2009. p. 459–510. https://doi.org/10.1016/B978-0-12-373660-4.00022-3.
21. León-Martínez FM, Rodríguez-Ramírez J, Medina-Torres LL, Méndez Lagunas LL, Bernad-Bernad MJ. Effects of drying conditions on the rheological properties of reconstituted mucilage solutions (Opuntia ficus-indica). Carbohydr Polym. 2011;84(1):439–45. https://doi.org/10.1016/j.carbpol.2010.12.004.
22. Rodríguez-Hernández GR, González-García R, Grajales-Lagunes A, Ruiz-Cabrera MA, Abud-Archila M. Spray-drying of cactus pear juice (*Opuntia streptacantha*): effect on the physicochemical properties of powder and reconstituted product. Dry Technol. 2005;23(4):955–73. https://doi.org/10.1080/DRT-200054251.
23. Moser P, Ferreira S, Nicoletti VR. Buriti oil microencapsulation in chickpea protein-pectin matrix as affected by spray drying parameters. Food Bioprod Process. 2019;117:183–93. https://doi.org/10.1016/j.fbp.2019.07.009.
24. Ruano Uscategui DC, Ciro Velásquez HJ, Sepúlveda Valencia JU. Concentrates of sugarcane juice and whey protein: study of a new powder product obtained by spray drying of their combinations. Powder Technol. 2018;333:429–38. https://doi.org/10.1016/j.powtec.2018.04.025.
25. Finney J, Buffo R, Reineccius GA. Effects of type of atomization and processing temperatures on the physical properties and stability of spray-dried flavors. J Food Sci. 2002;67(3):1108–14. https://doi.org/10.1111/j.1365-2621.2002.tb09461.x.
26. Tonon RV, Brabet C, Pallet D, Brat P, Hubinger MD. Physicochemical and morphological characterisation of açai (Euterpe oleraceae Mart.) powder produced with different carrier agents. Int J Food Sci Technol. 2009;44(10):1950–8. https://doi.org/10.1111/j.1365-2621.2009.02012.x.
27. Yoganandi J, Mehta BM, Wadhwani KN, Darji VB, Aparnathi KD. Evaluation and comparison of camel milk with cow milk and buffalo milk for gross composition. J Camel Pract Res. 2014;21(2):259–65. https://doi.org/10.5958/2277-8934.2014.00046.0.
28. Schröder J, Kraus S, Rocha BB, Gaukel V, Schuchmann HP. Characterization of gelatinized corn starch suspensions and resulting drop size distributions after effervescent atomization. J Food Eng. 2011;105(4):656–62. https://doi.org/10.1016/j.jfoodeng.2011.03.028.
29. Finotello G, Kooiman RF, Padding JT, Buist KA, Jongsma A, Innings F, Kuipers JAM. The dynamics of milk droplet–droplet collisions. Exp Fluids. 2017;59(1):1–19. https://doi.org/10.1007/s00348-017-2471-2.
30. Mensink MA, Frijlink HW, van der Voort MK, Hinrichs WLJ. Inulin, a flexible oligosaccharide I: review of its physicochemical characteristics. Carbohydr Polym. 2015;130:405–19. https://doi.org/10.1016/j.carbpol.2015.05.026.
31. Bhusari SN, Muzaffar K, Kumar P. Effect of carrier agents on physical and microstructural properties of spray dried tamarind pulp powder. Powder Technol. 2014;266:354–64. https://doi.org/10.1016/j.powtec.2014.06.038.
32. Bhandari BR, Datta N, Howes T. Problems associated with spray drying of sugar-rich foods. Dry Technol. 1997;15(2):671–84. https://doi.org/10.1080/07373939708917253.
33. Wang Y, Wang B, Selomulya C. Dairy encapsulation systems by atomization-based technology. In: Juliano P, Buckow R, Nguyen MH, Knoerzer K, Sellahewa J, editors. Food engineering innovations across the food supply Chain. Cambridge: Academic Press; 2022. p. 247–60. https://doi.org/10.1016/B978-0-12-821292-9.00023-6.
34. Wittner MO, Karbstein HP, Gaukel V. Energy efficient spray drying by increased feed dry matter content: investigations on the applicability of air-core-liquid-ring atomization on pilot scale. Dry Technol. 2019;38(10):1323–31. https://doi.org/10.1080/07373937.2019.1635616.
35. Stähle P, Gaukel V, Schuchmann HP. Investigation on the applicability of the effervescent atomizer in spray drying of foods: influence of liquid viscosity on nozzle internal two-phase flow and spray characteristics. J Food Process Eng. 2014;38(5):474–87. https://doi.org/10.1111/jfpe.12178.
36. Lefebvre AH, McDonell VG. Atomization and sprays. 2nd ed. Boca Raton: CRC Press; 2017. https://doi.org/10.1201/9781315120911.
37. Heydari A, Goharimanesh M, Gharib M, Koochi A. Modeling the ultrasonic atomization process of milk and powder production using spray drying method. IFSTRJ. 2023;19(1):145–68. https://doi.org/10.22067/ifstrj.2022.75615.1154.
38. Habtegebriel H, Wawire M, Gaukel V, Taboada ML. Comparison of the viscosity of camel milk with model milk systems in relation to their atomization properties. J Food Sci. 2020;85(10):3459–66. https://doi.org/10.1111/1750-3841.15451.
39. Saha D, Nanda SK, Yadav DN. Optimization of spray drying process parameters for production of groundnut milk powder. Powder Technol. 2019;355:417–24. https://doi.org/10.1016/j.powtec.2019.07.066.
40. Taboada ML, Heiden-Hecht T, Brückner-Gühmann M, Karbstein HP, Drusch S, Gaukel V. Spray drying of emulsions: Influence of the emulsifier system on changes in oil droplet size during the drying step. J Food Process Preserv. 2021;45(9):e15753. https://doi.org/10.1111/jfpp.15753.
41. Guildenbecher DR, López-Rivera C, Sojka PE. Secondary atomization. Exp Fluids. 2009;46(3):371–402. https://doi.org/10.1007/s00348-008-0593-2.
42. Serfert Y, Schröder J, Mescher A, Laackmann J, Rätzke K, Shaikh MQ, Gaukel V, Moritz HU, Schuchmann HP, Walzel P, Drusch S, Schwarz K. Spray drying behaviour and functionality of emulsions with β-lactoglobulin/pectin interfacial complexes. Food Hydrocoll. 2013;31(2):438–45. https://doi.org/10.1016/j.foodhyd.2012.11.037.

43. Taneja A, Ye A, Jones JR, Archer R, Singh H. Behaviour of oil droplets during spray drying of milk-protein-stabilised oil-in-water emulsions. Int Dairy J. 2013;28(1):15–23. https://doi.org/10.1016/j.idairyj.2012.08.004.
44. Drapala KP, Auty MAE, Mulvihill DM, O'Mahony JA. Influence of emulsifier type on the spray-drying properties of model infant formula emulsions. Food Hydrocoll. 2017;69:56–66. https://doi.org/10.1016/j.foodhyd.2016.12.024.
45. Matsumiya K, Takahashi Y, Nakanishi K, Dotsu N, Matsumura Y. Diglycerol esters of fatty acids promote severe coalescence between protein-stabilized oil droplets by emulsifier–protein competitive interactions. Food Hydrocoll. 2014;42:397–402. https://doi.org/10.1016/j.foodhyd.2014.03.002.
46. Tatar Turan F, Kahyaoglu T. The effect of an ultrasonic spray nozzle on carbohydrate and protein-based coating materials for blueberry extract microencapsulation. J Sci of Food and Agric. 2021;101(1):120–30. https://doi.org/10.1002/jsfa.10622.
47. Anandharamakrishnan C, Ishwarya SP. Spray drying techniques for food ingredient encapsulation. 1st ed. Hoboken: Wiley; 2015. https://doi.org/10.1002/9781118863985.
48. López-Díaz AS, Méndez-Lagunas LL. Mucilage-based films for food applications. Food Rev Int. 2022;39(9):6677–706. https://doi.org/10.1080/87559129.2022.2123501.
49. Suhag R, Kumar N, Petkoska AT, Upadhyay A. Film formation and deposition methods of edible coating on food products: a review. Food Res Int. 2020;136:109582. https://doi.org/10.1016/j.foodres.2020.109582.
50. Poverenov E, Zaitsev Y, Arnon H, Granit R, Alkalai-Tuvia S, Perzelan Y, Weinberg T, Fallik E. Effects of a composite chitosan–gelatin edible coating on postharvest quality and storability of red bell peppers. Postharvest Biol Technol. 2014;96:106–9. https://doi.org/10.1016/j.postharvbio.2014.05.015.
51. Saberi B, Golding JB, Marques JR, Pristijono P, Chockchaisawasdee S, Scarlett CJ, Stathopoulos CE. Application of biocomposite edible coatings based on pea starch and guar gum on quality, storability and shelf life of 'Valencia' oranges. Postharvest Biol Technol. 2018;137:9–20. https://doi.org/10.1016/j.postharvbio.2017.11.003.
52. Al-Naamani L, Dutta J, Dobretsov S. Nanocomposite zinc oxide-chitosan coatings on polyethylene films for extending storage life of Okra (Abelmoschus esculentus). Nanomater. 2018;8(7):479. https://doi.org/10.3390/nano8070479.
53. Atieno L, Owino W, Ateka EM, Ambuko J. Influence of coating application methods on the postharvest quality of cassava. Int J Food Sci. 2019;2019:e2148914. https://doi.org/10.1155/2019/2148914.
54. Chiu PE, Lai LS. Antimicrobial activities of tapioca starch/decolorized hsian-tsao leaf gum coatings containing green tea extracts in fruit-based salads, romaine hearts and pork slices. Int J Food Microbiol. 2010;139(1):23–30. https://doi.org/10.1016/j.ijfoodmicro.2010.01.010.
55. Antoniewski MN, Barringer SA, Knipe CL, Zerby HN. Effect of a gelatin coating on the shelf life of fresh meat. J Food Sci. 2007;72(6):E382–7. https://doi.org/10.1111/j.1750-3841.2007.00430.x.
56. Hanumantharaju KN, Thangavel K, Poornima DS, Ganapathy S, Jesudas DM. Development of electrostatic spray coating machine for edible coating of fruits. Ann Agri Bio Res. 2022;27(2):231–7.
57. Khan MKI, Schutyser MAI, Schroën K, Boom R. The potential of electrospraying for hydrophobic film coating on foods. J Food Eng. 2012;108(3):410–6. https://doi.org/10.1016/j.jfoodeng.2011.09.005.
58. Andrade RD, Skurtys O, Osorio FA. Atomizing spray systems for application of edible coatings. Compr Rev Food Sci Food Saf. 2012;11(3):323–37. https://doi.org/10.1111/j.1541-4337.2012.00186.x.
59. Rizkalla AA, Lefebvre AH. The influence of air and liquid properties on airblast atomization. J Fluids Eng. 1975;97(3):316–20. https://doi.org/10.1115/1.3447309.
60. Schick RJ. Spray Technology Reference Guide: Understanding Drop Size. Spraying Systems Co.; 2008. Bulletin No. 459C
61. Jayaprakash P, Maudhuit A, Gaiani C, Desobry S. Encapsulation of bioactive compounds using competitive emerging techniques: Electrospraying, nano spray drying, and electrostatic spray drying. J Food Eng. 2023;339:111260. https://doi.org/10.1016/j.jfoodeng.2022.111260.
62. Ré M I. Microencapsulation by spray drying. Dry Technol. 1998;16(6):1195–236. https://doi.org/10.1080/07373939808917460.
63. Linke A, Weiss J, Kohlus R. Factors determining the surface oil concentration of encapsulated lipid particles: impact of the emulsion oil droplet size. Eur Food Res Technol. 2020;246(10):1933–43. https://doi.org/10.1007/s00217-020-03545-5.
64. Oikonomopoulou V, Stramarkou M, Plakida A, Krokida M. Optimization of encapsulation of stevia glycosides through electrospraying and spray drying. Food Hydrocoll. 2022;131: 107854. https://doi.org/10.1016/j.foodhyd.2022.107854.
65. Taboada ML, Schäfer AC, Karbstein HP, Gaukel V. Oil droplet breakup during pressure swirl atomization of food emulsions: Influence of atomization pressure and initial oil droplet size. J Food Process Eng. 2020;44(1): e13598. https://doi.org/10.1111/jfpe.13598.
66. Zhang Y, Yuan S, Wang L. Investigation of capillary wave, cavitation and droplet diameter distribution during ultrasonic atomization. Exp Therm Fluid Sci. 2021;120: 110219. https://doi.org/10.1016/j.expthermflusci.2020.110219.
67. Antonio-Gutiérrez O, López-Díaz AS, Mani-López E, Palou E, López-Malo A, Ramírez-Corona N. Insights on the effectiveness of pneumatic and ultrasonic atomization in combination with UVC light for processing of fruit juices. J Food Sci Technol. 2022;59(7):2925–30. https://doi.org/10.1007/s13197-022-05468-3.
68. Mohammed M, Alqahtani N, El-Shafie H. Development and evaluation of an ultrasonic humidifier to control humidity in a cold storage room for postharvest quality management of dates. Foods. 2021;10(5):949. https://doi.org/10.3390/foods10050949.
69. Kishimoto T, Kadota K, Furukawa R, Tozuka Y, Shimosaka A, Shirakawa Y. Nozzleless electrostatic atomization process for crystallization via liquid-liquid interfaces. J Chem Eng Japan. 2017;50(5):367–75. https://doi.org/10.1252/jcej.16we236.
70. Sadri B, Hokmabad BV, Esmaeilzadeh E, Gharraei R. Experimental investigation of electrosprayed droplets behaviour of water and KCl aqueous solutions in silicone oil. Exp Therm Fluid Sci. 2012;36:249–55. https://doi.org/10.1016/j.expthermflusci.2011.09.021.
71. Kikuchi K, Kadota K, Tozuka Y, Shimosaka A, Yoshida M, Shirakawa Y. Effects of the process parameters on the size distribution of taurine particles produced by nozzleless electrostatic atomization. Chem Eng Process. 2017;117:38–44. https://doi.org/10.1016/j.cep.2017.03.015.
72. Mori C, Kadota K, Tozuka Y, Shimosaka A, Yoshida M, Shirakawa Y. Application of nozzleless electrostatic atomization to encapsulate soybean oil with solid substances. J Food Eng. 2019;246:25–32. https://doi.org/10.1016/j.jfoodeng.2018.10.023.

73. Mohammadi-Aragh MK, Linhoss JE, Evans JD. Effects of various disinfectants on the bacterial load and microbiome of broiler hatching eggs using electrostatic spray1. J Appl Poult Res. 2022;31(3): 100278. https://doi.org/10.1016/j.japr.2022.100278.
74. Jiang W, Etienne X, Li K, Shen C. Comparison of the efficacy of electrostatic versus conventional sprayer with commercial antimicrobials to inactivate salmonella, Listeria monocytogenes, and Campylobacter jejuni for eggs and economic feasibility analysis. J Food Prot. 2018;81(11):1864–70. https://doi.org/10.4315/0362-028X.JFP-18-249.
75. Ganesh V, Hettiarachchy NS, Ravichandran M, Johnson MG, Griffis CL, Martin EM, Meullenet JF, Ricke SC. Electrostatic sprays of food-grade acids and plant extracts are more effective than conventional sprays in decontaminating Salmonella typhimurium on spinach. J Food Sci. 2010;75(9):M574–9. https://doi.org/10.1111/j.1750-3841.2010.01859.x.
76. Lee CH, Woo HJ, Kang JH, Song KB. Electrostatic spraying of passion fruit (Passiflora edulis L.) peel extract for inactivation of Escherichia coli O157:H7 and Listeria monocytogenes on fresh-cut Lollo Rossa and beetroot leaves. Food Bioproc Tech. 2021;14(5):898–908. https://doi.org/10.1007/s11947-021-02608-z.
77. Písecký J. Handbook of milk powder manufacture. Düsseldorf: GEA Niro; 2012.
78. Sarrate R, Ticó JR, Miñarro M, Carrillo C, Fàbregas A, García-Montoya E, Pérez-Lozano P, Suñé-Negre JM. Modification of the morphology and particle size of pharmaceutical excipients by spray drying technique. Powder Technol. 2015;270:244–55. https://doi.org/10.1016/j.powtec.2014.08.021.
79. Filková I, Mujumdar AS. Industrial spray drying systems. In: Mujumdar AS, editor. Handbook of industrial drying: second edition, revised and expanded, vol. 1. CRC Press; 2019. p. 263–307.
80. Akafuah NK. Automotive paint spray characterization and visualization. In: Toda K, Salazar A, Saito K, editors. Automotive painting technology: a monozukuri-hitozukuri perspective. Dordrecht: Springer; 2013.
81. Hede PD, Bach P, Jensen AD. Two-fluid spray atomisation and pneumatic nozzles for fluid bed coating/agglomeration purposes: a review. Chem Eng Sci. 2008;63(14):3821–42. https://doi.org/10.1016/j.ces.2008.04.014.
82. Konstantinov D, Marsh R, Bowen PJ, Crayford A. Effervescent atomization for industrial energy–technology review. At Sprays. 2010;20(6):525–52. https://doi.org/10.1615/atomizspr.v20.i6.40.
83. Jedelský J, Otahal J, Jicha M. Effervescent atomizer: influence of the internal ge ometry on atomization performance. In: 21st ILASS-Europe; 2007.
84. Rizkalla AA. The Influence of Air and Liquid Properties on Airblast Atomization. Doctoral dissertation. Cranfield University; 1974. https://dspace.lib.cranfield.ac.uk/handle/1826/11924
85. Simmons HC. The correlation of drop-size distributions in fuel nozzle sprays—part I: the drop-size/volume-fraction distribution. J Eng Power. 1977;99(3):309–14. https://doi.org/10.1115/1.3446488.
86. Nath S, Satpathy GR. A systematic approach for investigation of spray drying processes. Dry Technol. 1998;16(6):1173–93. https://doi.org/10.1080/07373939808917459.
87. Barreras F, Lozano A, Barroso J, Lincheta E. Experimental characterization of industrial twin-fluid atomizers. Sprays. 2006;16(2):127–46. https://doi.org/10.1615/atomizspr.v16.i2.10.
88. Nukiyama S, Tanasawa Y. An experiment on the atomization of liquid: 4th report, the effect of the properties of liquid on the size of drops. Trans Jpn Soc Mech Eng. 1939;5(18):136–43. https://doi.org/10.1299/kikai1938.5.136.
89. Lorenzetto GE, Lefebvre AH. Measurements of drop size on a plain-jet airblast atomizer. AIAA J. 1977;15(7):1006–10. https://doi.org/10.2514/3.60742.
90. Jasuja AK. Plain-Jet Airblast Atomization of Alternative Liquid Petroleum Fuels Under High Ambient Air Pressure Conditions. In: American Society of Mechanical Engineers Digital Collection; 1982. https://doi.org/10.1115/82-GT-32
91. Rizk NK, Lefebvre AH. Spray Characteristics of Plain-Jet Airblast Atomizers. In: American Society of Mechanical Engineers Digital Collection; 1983. https://doi.org/10.1115/83-gt-138
92. Nguyen DA, Rhodes MJ. Producing fine drops of water by twin-fluid atomisation. Powder Technol. 1998;99(3):285–92. https://doi.org/10.1016/s0032-5910(98)00125-9.
93. Sojka PE, Lefebvre AH. A Novel Method of Atomizing Coal-Water Slurry Fuels. Thermal Sciences and Propulsion Center. School of Mechanical Engineering. Purdue University; 1990. https://doi.org/10.2172/6581179
94. Sovani SD, Sojka PE, Lefebvre AH. Effervescent atomization. Prog Energy Combust Sci. 2001;27(4):483–521. https://doi.org/10.1016/s0360-1285(00)00029-0.
95. Omer K, Ashgriz N. Spray nozzles. In: Ashgriz N, editor. Handbook of atomization and sprays: theory and applications. Boston: Springer; 2011. https://doi.org/10.1007/978-1-4419-7264-4_24.
96. Sutherland JJ, Sojka PE, Plesniak MW. Ligament-controlled effervescent atomization. At Sprays. 1997;7(4):383–406. https://doi.org/10.1615/atomizspr.v7.i4.40.
97. Sovani SD, Sojka PE, Sivathanu YR. Prediction of drop size distributions from first principles: the influence of fluctuations in relative velocity and liquid physical properties. At Sprays. 1999;9(2):133–52. https://doi.org/10.1615/atomizspr.v9.i2.20.
98. Qian L, Lin J, Xiong H. A fitting formula for predicting droplet mean diameter for various liquid in effervescent atomization spray. J Therm Spray Technol. 2010;19(3):586–601. https://doi.org/10.1007/s11666-009-9457-4.
99. Simmons HC. The prediction of sauter mean diameter for gas turbine fuel nozzles of different types. J Eng Power. 1980;102(3):646–52. https://doi.org/10.1115/1.3230318.
100. Polikhov SA. Experimental Study of Subcritical to Supercritical Mixing. Doctoral dissertation. University of Florida; 2007. https://ufdc.ufl.edu/UFE0021034/00001/citation
101. Jasuja AK. Atomization of crude and residual fuel oils. J Eng Power. 1979;101(2):250–8. https://doi.org/10.1115/1.3446480.
102. El-Shanawany MS, Lefebvre AH. Airblast atomization: effect of linear scale on mean drop size. J Energy. 1980;4(4):184–9. https://doi.org/10.2514/3.62472.
103. Lefebvre AH. Energy considerations in twin-fluid atomization. J Eng Gas Turbine Power. 1992;114(1):89–96. https://doi.org/10.1115/1.2906311.
104. Beck JE, Lefebvre AH, Koblish TR. Airblast atomization at conditions of low air velocity. J Propuls Power. 1991;7(2):207–12. https://doi.org/10.2514/3.23313.

105. Gretzinger J, Marshall WR Jr. Characteristics of pneumatic atomization. AIChE J. 1961;7(2):312–8. https://doi.org/10.1002/aic.690070229.
106. Kim KY, Marshall JRWR. Drop-size distributions from pneumatic atomizers. AIChE J. 1971;17(3):575–84. https://doi.org/10.1002/aic.690170318.
107. Sander A, Penović T. Droplet size distribution obtained by atomization with two-fluid nozzles in a spray dryer. Chem Eng Technol. 2014;37(12):2073–84. https://doi.org/10.1002/ceat.201400185.
108. Wood RW, Loomis AL. XXXVIII. The physical and biological effects of high-frequency sound-waves of great intensity. Lond Edinb Dublin Philos Mag J Sci. 1927;4(22):417–436. https://doi.org/10.1080/14786440908564348
109. Söllner K. The mechanism of the formation of fogs by ultrasonic waves. Trans Faraday Soc. 1936;32:1532–6. https://doi.org/10.1039/tf9363201532.
110. Kudo T, Sekiguchi K, Sankoda K, Namiki N, Nii S. Effect of ultrasonic frequency on size distributions of nanosized mist generated by ultrasonic atomization. Ultrason Sonochem. 2017;37:16–22. https://doi.org/10.1016/j.ultsonch.2016.12.019.
111. Rayleigh JWS. The theory of sound, vol. 2. Mineola: Dover Publications; 1945.
112. Lang RJ. Ultrasonic atomization of liquids. J Acoust Soc Am. 1962;34(1):6–8. https://doi.org/10.1121/1.1909020.
113. Lobdell DD. Particle size-amplitude relations for the ultrasonic atomizer. J Acoust Soc Am. 1968;43(2):229–31. https://doi.org/10.1121/1.1910770.
114. Yasuda K, Bando Y, Yamaguchi S, Nakamura M, Oda A, Kawase Y. Analysis of concentration characteristics in ultrasonic atomization by droplet diameter distribution. Ultrason Sonochem. 2005;12(1–2):37–41. https://doi.org/10.1016/j.ultsonch.2004.05.008.
115. Peskin RL, Raco RJ. Ultrasonic atomization of liquids. J Acoust Soc Am. 1963;35(9):1378–81. https://doi.org/10.1121/1.1918700.
116. Dobre M, Bolle L. Practical design of ultrasonic spray devices: experimental testing of several atomizer geometries. Exp Therm Fluid Sci. 2002;26(2–4):205–11. https://doi.org/10.1016/s0894-1777(02)00128-0.
117. Rajan R, Pandit AB. Correlations to predict droplet size in ultrasonic atomisation. Ultrasonics. 2001;39(4):235–55. https://doi.org/10.1016/s0041-624x(01)00054-3.
118. Avvaru B, Patil MN, Gogate PR, Pandit AB. Ultrasonic atomization: effect of liquid phase properties. Ultrasonics. 2006;44(2):146–58. https://doi.org/10.1016/j.ultras.2005.09.003.
119. Barba AA, d'Amore M, Cascone S, Lamberti G, Titomanlio G. Intensification of biopolymeric microparticles production by ultrasonic assisted atomization. Chem Eng Process. 2009;48(10):1477–83. https://doi.org/10.1016/j.cep.2009.08.004.
120. Lide DR. CRC handbook of chemistry and physics: a ready-reference book of chemical and physical data. 86th ed. Boca Raton: CRC Press; 2005.
121. Sindayihebura D, Bolle L, Cornet A, Joannes L. Theoretical and experimental study of transducers aimed at low-frequency ultrasonic atomization of liquids. J Acoust Soc Am. 1998;103(3):1442–8. https://doi.org/10.1121/1.421300.
122. Sugondo A, Sutrisno Anggono W, Anne O. Effect of frequency on droplet characteristics in ultrasonic atomization process. ES Web Conf. 2019;130:01002. https://doi.org/10.1051/e3sconf/201913001002.